

Manuscript Details

Manuscript number	DYPI_2017_2138_R2
Title	Pyrene-based color-tunable dipolar molecules: synthesis, characterization and optical properties
Article type	Research paper

Abstract

A controllable regioselective approach to achieve dipolar functionalization at the active sites (1,3-positions) and K-region (5,9-positions) of pyrene is demonstrated. Following this strategy, a set of dipolar 1,3-diphenyl-5,9-di(4-R-phenylethynyl)pyrenes were synthesized and systematically investigated by ¹H/¹³C NMR spectroscopy, X-ray crystallography, electronic spectra, as well as by theoretical calculations. Especially, by adjusting the substituents at the 5,9-positions of pyrene, the pyrene-based dipolar molecules 4 exhibit tunable optical properties with a wide emission band from blue to orange-red.

Keywords	regioselective synthesis; pyrene chemistry; K-region; tunable emission; dipolar molecules
Corresponding Author	Takehiko Yamato
Corresponding Author's Institution	Saga University
Order of Authors	Chuan-Zeng Wang, Xing Feng, Zannatul Kowser, Chong Wu, Thamina Akther, Mark R.J. Elsegood, Carl Redshaw, Takehiko Yamato
Suggested reviewers	hu jianyong, Ben Tang, Qichun Zhang, G. Richard Stephenson, Todd Marder, Erjun Zhou

Submission Files Included in this PDF

File Name [File Type]

- 7. 0103 Cover letter.doc [Cover Letter]
- 0103 Response to reviewers.docx [Response to Reviewers]
- 2. 1219 Highlights.docx [Highlights]
- 6. 1218 Graphical Abstract.docx [Graphical Abstract]
- 1. 0103 Text R2 .docx [Manuscript File]
- 3. 1219 Scheme and Figures.docx [Figure]
- 4. 1219 Tables.docx [Table]
- 5. 1219 Supporting Information R1 .pdf [Data in Brief]
- 9. 4c-checkcif.pdf [Data in Brief]

Submission Files Not Included in this PDF

File Name [File Type]

- 9. 4c.cif [Data in Brief]

To view all the submission files, including those not included in the PDF, click on the manuscript title on your EVISE Homepage, then click 'Download zip file'.

Dear Prof. Yoon,

We are resubmitting the manuscript ID: DYPI_2017_2138_R1, entitled “**Pyrene-based color-tunable dipolar molecules: synthesis, characterization and optical properties**” to *Dyes and Pigments*. This revision was carefully carried out according to the suggestion of the reviewer 3. We hope that these changes will satisfy the reviewer.

The manuscript mainly presents an innovative, facile, and promising controllable regioselective strategy for the asymmetric functionalization at the active sites (1,3-positions) and the K-region (5,9-positions) of pyrene. This methodology is not only useful in the construction of novel asymmetrical dipolar molecules based on pyrene and polycyclic aromatic hydrocarbons (PAHs), but it could also enable to construction of new asymmetric pyrene-based organic luminogens with wide-range color tuning. Herein, a set of asymmetric 1,3-diphenyl-5,9-diarylethynyl pyrenes are synthesized and investigated by $^1\text{H}/^{13}\text{C}$ NMR spectroscopy, X-ray crystallography, electronic spectra, as well as by theoretical calculations. Further, by adjusting the substituents at the 5,9-positions of pyrene, the asymmetric pyrene-based molecules exhibit wide visible emission from blue to orange-red. As the fundamental science behind the synthetic strategy, and photophysical properties is developed, which will open the door to the preparation of more attractive pyrene-based luminescence materials. More importantly, it is helpful to understand the mechanism between the molecular structures and photophysical properties.

This article has not been published elsewhere in whole or in part. All authors have read and approved the content, and agree to submit for consideration for publication in the journal. There are no any ethical/legal conflicts involved in the article.

Your consideration of this manuscript is highly appreciated, and hopefully our paper is a worthwhile addition to your journal.

Yours faithfully,

Prof. Dr. Takehiko Yamato (corresponding author)

Department of Applied Chemistry, Faculty of Science and Engineering, Saga University

Honjo-machi 1, Saga-shi, Saga 840-8502, Japan

Fax: (internet.) + 81(0)952/28-8548

E-mail: yamatot@cc.saga-u.ac.jp

Manuscript number: DYPI_2017_2138_R1

Title: Pyrene-based color-tunable dipolar molecules: synthesis, characterization and optical properties

Journal: Dyes and Pigments

Correspondence Author: Prof. Dr. Takehiko Yamato

COMMENTS TO AUTHOR:

-Reviewer 3

The revised paper still needs a few minor corrections before acceptance.

- (1) 1. Line 378: replace "One suitable single crystal of 4c was obtained in mixture solution" replace by " A crystal of 4csuitable for X-ray diffraction study was obtained from CHCl₃ /hexane solution ".

Response: Thank you very much for your suggestion, we have changed this sentence in the revised version.

- (2) 2. Line 488: replace "molecular" by "molecule".

Response: we changed “molecular” to “molecule”.

- (3) 3. Line 499: replace "from the pyrene core to both C₆H₄OMe rings" by "between the pyrene core and both C₆H₄OMe rings"

Response: Thank you very much for your suggestion, we have changed this sentence in the revised version.

- (4) 4. Line 638: replace "dimethyl formamide" by "dimethylformamide"

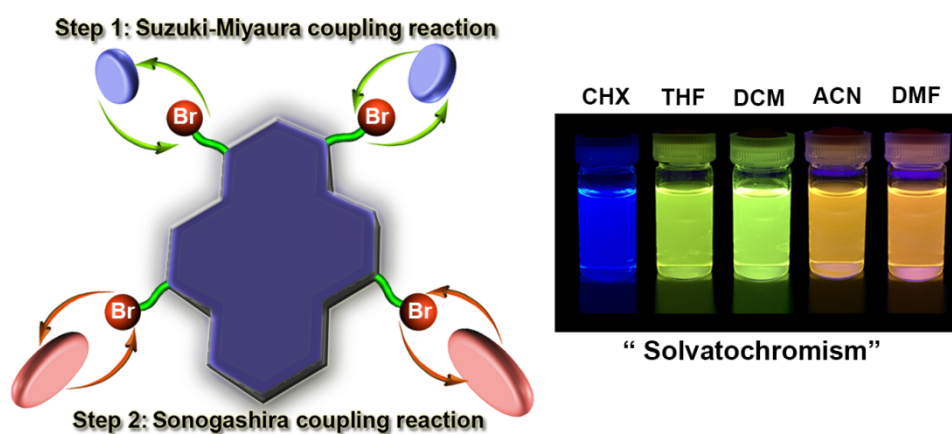
Response: Thank you very much for your suggestion, we have improved this word in the revised version.

1. Controllable regioselective strategy for the asymmetric functionalization at the active sites and the K-region of pyrene.
2. This type molecules exhibited thermal stability ($> 256\text{ }^{\circ}\text{C}$) and wide-range color tuning ($> 100\text{ nm}$)
3. All the compounds exhibited high quantum yield in organic solution.

Pyrene-based color-tunable dipolar molecules: synthesis, characterization and optical properties

Chuan-Zeng Wang ^a, Xing Feng ^{b,*}, Zannatul Kowser ^{a,c}, Chong Wu ^a, Thamina Akther ^a, Mark R.J. Elsegood ^d, Carl Redshaw ^e, Takehiko Yamato ^{a,*}

A set of dipolar molecules 1,3-diphenyl-5,9-diarylethynyl)pyrenes which exhibit a wide visible emission ranging from blue to orange-red were synthesized by employing a controllable regioselective approach at the active sites and K-region of pyrene.



Pyrene-based color-tunable dipolar molecules: synthesis, characterization and optical properties

Chuan-Zeng Wang ^a, Xing Feng ^{b,*}, Zannatul Kowser ^{a,c}, Chong Wu ^a, Thamina Akther ^a, Mark R.J. Elsegood ^d, Carl Redshaw ^e, Takehiko Yamato ^{a,*}

^a Department of Applied Chemistry, Faculty of Science and Engineering, Saga University Honjo-machi 1, Saga 840-8502

^b Faculty of Material and Energy Engineering, Guangdong University of Technology, Guangzhou 510006, China

^c International University of Business Agriculture and Technology. Dhaka, 1230. Bangladesh

^d Chemistry Department, Loughborough University, Loughborough, LE11 3TU, UK

^e Department of Chemistry, School of Mathematics and Physical Sciences, The University of Hull, Cottingham Road, Hull, Yorkshire HU6 7RX, UK

*Corresponding author

E-mail: yamatot@cc.saga-u.ac.jp, hyxhn@sina.com

ABSTRACT: A controllable regioselective approach to achieve dipolar functionalization at the active sites (1,3-positions) and K-region (5,9-positions) of pyrene is demonstrated. Following this strategy, a set of dipolar 1,3-diphenyl-5,9-di(4-R-phenylethynyl)pyrenes were synthesized and systematically investigated by ¹H/¹³C NMR spectroscopy, X-ray crystallography, electronic spectra, as well as by theoretical calculations. Especially, by adjusting the substituents at the 5,9-positions of pyrene, the pyrene-based dipolar molecules **4** exhibit tunable optical properties with a wide emission band from blue to orange-red.

Keywords: Regioselective Synthesis; Pyrene Chemistry; K-region; Tunable Emission; Dipolar Molecules

1. Introduction

The design and synthesis of tunable emission materials have been an attractive research topic in both academic and commercial arenas, for example, multicolored emission materials have an extremely wide range of potential applications in light emitting displays [1], multicolor lasers [2], and organic light emitting diodes (OLEDs) [3]. On the other hand, the construction of novel fluorophores with tunable emission colors is achieved by adjusting the structure and

60
61
62
63 thereby altering the transition-energy levels as evidenced by chemical/physical methods [4].
64 Generally, most strategies have relied on fine-tuning of the host materials for the wide-range
65 altering of the emission colors, which involves the introduction of various electron donating or
66 withdrawing groups to the host compounds [5], tuning the intramolecular charge-transfer [6]
67 or molecular weight (for polymers) [7] or by voltage-controlled electroluminescence (EL)
68 technology [8]. Nevertheless, to achieve a tunable emission material with satisfactory
69 properties for high-performance devices remains a challenge. Moreover, understanding of the
70 underlying structure-property relationship of such systems is still a topic of on-going interest.
71 For conventional organic synthetic approaches, push-pull chromophores (dipolar molecules)
72 play a significant role in constructing tunable emission molecules which can exhibit a wide
73 emission range from deep blue to red, and even to the near infrared (NIR) region [6,9].
74
75
76
77
78
79
80
81
82

83 Generally, the pyrene exhibits strong positional dependence along the long *Y*-axis (the active
84 site of 1-, 3-, 6- and 8- positions and plane node of 2,7-positions) and the short *Z*-axis (K-region
85 of 4-, 5-, 9- and 10-positions). Theory and experimental studies show that the substitution
86 position can affect the intramolecular electron-transfer process [10]. Theoretically, since the $S_1 \leftarrow S_0$
87 and $S_3 \leftarrow S_0$ transitions are polarized along the short axis of pyrene, introducing
88 appropriate moieties into the K-region of pyrene may lead to a distinct change of the energy of
89 the $S_1 \leftarrow S_0$ and $S_3 \leftarrow S_0$ excitations [10]. While our experiment confirmed pyrenes derivatives
90 show a significant effect to the emission with large red-shifted depending on the position-
91 substitution at the long axis or K-regions [11]. So, it seems that the pyrene-based dipolar
92 molecules would exhibit interesting optical properties when functionalization of pyrene both
93 at long axis and K-regions has occurred [12].
94
95
96
97
98
99
100
101
102

103 To date, there are challenging issues regarding controllable regioselectivity for modifying
104 the pyrene core. In an effort to conquer these difficulties, a number of reliable strategies were
105 established to modify the active sites of pyrene [13]. By contrast, functionalization at the K-
106 region of pyrene is attractive but difficult to carry out. Several attempts have been made to
107 exploit this region, including oxidation [14], bromination [15], nitration [16], formylation [17],
108 and borylation [18] reactions. However, multistep routes, low selectivity, and harsh conditions
109 have driven us to explore more effective strategies for regioselective substitution at the K-
110 region of pyrene.
111
112
113
114
115
116
117
118

2. Experimental section

2.1. General procedures

All reactions were carried out under a dry N₂ atmosphere. Solvents were Guaranteed reagent (GR) for cyclohexane, tetrahydrofuran (THF), dichloromethane (CH₂Cl₂), acetonitrile (CH₃CN), and dimethylformamide (DMF), and stored over molecular sieves. Other reagents were obtained commercially and used without further purification. Reactions were monitored using thin layer chromatography (TLC). Commercial TLC plates (Merck Co.) were developed and the spots were identified under UV light at 254 and 365 nm. Column chromatography was performed on silica gel 60 (0.063-0.200 mm). All synthesized compounds were characterized using ¹H-NMR and ¹³C-NMR spectroscopy, and by HRMS (FAB) mass analysis. Fluorescence spectroscopic studies were performed in various organic solvents in a semimicro fluorescence cell (Hellma®, 104F-QS, 10 × 4 mm, 1400 μL) with a Varian Cary Eclipse spectrophotometer. Fluorescence quantum yields were measured using absolute methods.

2.2. Synthetic Procedures

2.2.1. Synthesis of compounds **3**

A series of precursors **3a**, **3b**, **3c** were synthesized from 7-*tert*-butyl-1,3-diphenylpyrene **2** [19] with the corresponding equiv. of Br₂ in the presence of iron-powder. ¹H NMR spectra of these three precursors were investigated. We also carried out this type of reaction in the absence of iron powder, and only a trace amount of precursor **3a** was detected. In this work, preferred candidate **3b** was fully characterized by ¹H NMR spectroscopy and mass analysis.

2.2.2. Synthesis of 7-*tert*-butyl-1,3-diphenyl-5-bromopyrene **3a**

A mixture of 7-*tert*-butyl-1,3-diphenylpyrene **2** (0.5 g, 1.2 mmol), and Fe powder (0.1 g, 1.8 mmol) were added in CH₂Cl₂ (5 mL), and the mixture was stirred at room temperature for 15 minutes under an argon atmosphere. A solution of Br₂ (0.09 mL, 1.8 mmol) in CH₂Cl₂ (6 mL) was slowly added dropwise with stirring, and the mixture was continuously stirred for 24 h at room temperature. Then the mixture was quenched with a 10% aqueous solution of Na₂S₂O₃. The mixture solution was extracted with CH₂Cl₂ (2 × 20 mL), the organic layer was washed with water (2 × 10 mL) and brine (30 mL), and then the solution was dried (MgSO₄), and the solvents were evaporated. The crude compound was washed with hot hexane to obtained **3a** as

178
179
180
181 a light-yellow solid (381 mg, 65%). M.p. 110–112°C; ¹H NMR (400 MHz, CDCl₃): δ_H = 1.63
182 (s, 9H, *t*Bu), 7.48–7.53 (m, 2H, Ar-*H*), 7.57 (d, *J* = 7.7 Hz, 4H, Ar-*H*), 7.65–7.69 (m, 4H, Ar-
183 *H*), 7.96 (s, 1H, pyrene-*H*), 8.03 (d, *J* = 9.2 Hz, 1H, pyrene-*H*), 8.19 (d, *J* = 9.2 Hz, 1H, pyrene-
184 *H*), 8.27 (s, 1H, pyrene-*H*), 8.54 (s, 1H, pyrene-*H*), 8.66 (s, 1H, pyrene-*H*) ppm. Due to poor
185 solubility in organic solvents it was not further characterized by ¹³C NMR spectroscopy. FAB-
186 MS: *m/z* calcd for C₃₂H₂₅Br 488.1140 [M⁺]; found 488.1140 [M⁺].
187
188
189

2.2.3. Synthesis of 7-*tert*-butyl-1,3-diphenyl-5,9-dibromopyrene **3b**

190
191
192
193 A mixture of 7-*tert*-butyl-1,3-diphenylpyrene **2** (2.0 g, 4.8 mmol), and Fe powder (0.82 g,
194 14.4 mmol) were added in CH₂Cl₂ (30 mL), and the mixture was stirred at room temperature
195 for 15 minutes under an argon atmosphere. A solution of Br₂ (0.75 mL, 14.4 mmol) in CH₂Cl₂
196 (50 mL) was slowly added dropwise with stirring, and the mixture was continuously stirred for
197 24 h at room temperature. Then the mixture was quenched with a 10% aqueous solution of
198 Na₂S₂O₃. The mixture solution was extracted with CH₂Cl₂ (2 × 100 mL), the organic layer was
199 washed with water (2 × 50 mL) and brine (50 mL), and then the solution was dried (MgSO₄),
200 and the solvents were evaporated. The crude compound was washed with hot hexane to
201 obtained **3b** as a yellow solid, which was recrystallized from hexane:CHCl₃ (v/v=8:1) to afford
202 **3b** as a light yellow solid (2.3 g, 83%). M.p. 115–116°C; ¹H NMR (400 MHz, CDCl₃): δ_H =
203 1.64 (s, 9H, *t*Bu), 7.51–7.54 (m, 2H, Ar-*H*), 7.58 (t, *J* = 7.3 Hz, 4H, Ar-*H*), 7.64 (d, *J* = 7.4 Hz,
204 4H, Ar-*H*), 7.96 (s, 1H, pyrene-*H*), 8.53 (s, 2H, pyrene-*H*), 8.73 (s, 2H, pyrene-*H*) ppm. Due
205 to poor solubility in organic solvents it was not further characterized by ¹³C NMR spectroscopy.
206 FAB-MS: *m/z* calcd for C₃₂H₂₄Br₂ 568.0224 [M⁺]; found 568.0227 [M⁺].
207
208
209
210
211
212
213
214
215
216
217
218

2.2.4. Synthesis of 7-*tert*-butyl-1,3-di(*para*-bromophenyl)-5,9-dibromopyrene **3c**

219
220 A mixture of 7-*tert*-butyl-1,3-diphenylpyrene **2** (0.5 g, 1.2 mmol), and Fe powder (0.4 g, 7.2
221 mmol) were added in CH₂Cl₂ (10 mL), and the mixture was stirred at room temperature for 15
222 minutes under an argon atmosphere. A solution of Br₂ (0.55 mL, 11.1 mmol) in CH₂Cl₂ (30
223 mL) was slowly added dropwise with stirring, and the mixture was continuously stirred for 24
224 h at room temperature. Then the mixture was quenched with a 10% aqueous solution of
225 Na₂S₂O₃. The mixture solution was extracted with CH₂Cl₂ (2 × 30 mL), the organic layer was
226 washed with water (2 × 15 mL) and brine (50 mL), and then the solution was dried (MgSO₄),
227 and the solvents were evaporated. The crude compound was purified by column
228
229
230
231
232
233
234
235
236

237
238
239 chromatography eluting with a 1:6 CH₂Cl₂/hexane mixture to obtained **3c** as a yellow solid
240 (653 mg, 71%). M.p. 202–203°C; ¹H NMR (400 MHz, CDCl₃): δ_H = 1.64 (s, 9H, *t*Bu), 7.50
241 (d, *J* = 8.1 Hz, 4H, Ar-*H*), 7.72 (d, *J* = 8.2 Hz, 4H, Ar-*H*), 7.86 (s, 1H, pyrene-*H*), 8.45 (s, 2H,
242 (d, *J* = 8.1 Hz, 4H, Ar-*H*), 7.72 (d, *J* = 8.2 Hz, 4H, Ar-*H*), 7.86 (s, 1H, pyrene-*H*), 8.45 (s, 2H,
243 pyrene-*H*), 8.75 (s, 2H, pyrene-*H*) ppm. Due to poor solubility in organic solvents it was not
244 further characterized by ¹³C NMR spectroscopy. FAB-MS: *m/z* calcd for C₃₂H₂₂Br₄ 725.8414
245 [M⁺]; found 725.8414 [M⁺].
246
247

2.2.5. Synthesis of 7-*tert*-butyl-1,3-diphenyl-5,9-diarylethynylpyrenes (**4a–f**)

248
249 A series of compounds **4a–f** were synthesized from 7-*tert*-butyl-1,3-diphenyl-5,9-
250 dibromopyrene **3** with the corresponding aryl alkyne by a Sonogashira coupling reaction.
251

7-*tert*-Butyl-1,3-diphenyl-5,9-bis-(4'-cyanophenylethynyl)pyrene (**4d**)

252
253 A mixture of 7-*tert*-butyl-1,3-diphenyl-5,9-dibromopyrene **3** (150 mg, 0.26 mmol), 4-
254 cyanophenyl acetylene (100 mg, 0.79 mmol), PdCl₂(PPh₃)₃ (18 mg, 0.03 mmol), CuI (10 mg,
255 0.52 mmol), PPh₃ (8 mg, 0.03 mmol) were added to a degassed solution of Et₃N (6 mL) and
256 DMF (6 mL). The resulting mixture was stirred at 100 °C for 24 h. After it was cooled to room
257 temperature, the reaction was quenched with water. The mixture was extracted with CH₂Cl₂ (2
258 × 500 mL), the organic layer was washed with water (2 × 30 mL) and brine (30 mL), and then
259 the solution was dried (MgSO₄), and evaporated. The residue was purified by column
260 chromatography eluting with a 1:2 CH₂Cl₂/hexane mixture to give **4d** as a yellow floccule (115
261 mg, 66%). M.p. 351–353°C; ¹H NMR (400 MHz, CDCl₃): δ_H = 1.68 (s, 9H, *t*Bu), 7.52–7.56
262 (m, 2H, Ar-*H*), 7.62 (t, *J* = 7.5 Hz, 4H, Ar-*H*), 7.66–7.73 (m, 8H, Ar-*H*), 7.77 (d, *J* = 8.2 Hz,
263 4H, Ar-*H*), 8.00 (s, 1H, pyrene-*H*), 8.53 (s, 2H, pyrene-*H*), 8.86 (s, 2H, pyrene-*H*) ppm; ¹³C
264 NMR (100 MHz, CDCl₃): δ_C = 31.05, 34.76, 91.66, 92.13, 110.14, 110.81, 117.61, 117.98,
265 118.73, 120.75, 122.20, 124.22, 125.77, 126.03, 126.93, 127.26, 127.78, 128.57, 129.13,
266 129.26, 129.69, 129.81, 130.87, 131.20, 131.33, 131.61, 131.79, 132.12, 138.24, 139.30,
267 140.28, 149.23 ppm; FAB-MS: *m/z* calcd for C₅₀H₃₂N₂ 660.2565 [M⁺]; found 660.2565 [M⁺].
268
269
270
271
272
273
274
275
276
277
278
279
280
281
282
283
284

285 A similar procedure using phenylacetylene, 4-fluorophenyl acetylene, 4-methoxyphenyl
286 acetylene, 4-formylphenyl acetylene, 4-*N,N*-dimethylphenyl acetylene, was followed for the
287 synthesis of **4a–c**, and **4e**, **4f**.
288
289

290 7-*tert*-Butyl-1,3-diphenyl-5,9-bis-(phenylethynyl)pyrene **4a** was obtained as an orange solid
291 (recrystallized from hexane:CH₂Cl₂=3:1, 87 mg, 54%). M.p. 352–353°C; ¹H NMR (400 MHz,
292
293
294
295

296
297
298
299
300
301
302
303
304
305
306
307
308
309
310
311
312
313
314
315
316
317
318
319
320
321
322
323
324
325
326
327
328
329
330
331
332
333
334
335
336
337
338
339
340
341
342
343
344
345
346
347
348
349
350
351
352
353
354

CDCl₃): $\delta_{\text{H}} = 1.68$ (s, 9H, *t*Bu), 7.42 (t, $J = 7.7$ Hz, 6H, Ar-*H*), 7.53 (d, $J = 6.7$ Hz, 2H, Ar-*H*), 7.61 (t, $J = 7.5$ Hz, 4H, Ar-*H*), 7.70 (d, $J = 7.3$ Hz, 8H, Ar-*H*), 7.95 (s, 1H, pyrene-*H*), 8.48 (s, 2H, pyrene-*H*), 8.93 (s, 2H, pyrene-*H*) ppm; ¹³C NMR (100 MHz, CDCl₃): $\delta_{\text{C}} = 31.97, 35.64, 88.31, 94.69, 120.62, 121.80, 123.42, 124.67, 126.91, 127.57, 128.40, 128.48, 128.53, 128.56, 129.59, 129.79, 130.43, 130.65, 131.71, 138.30, 140.58, 149.87$ ppm; FAB-MS: m/z calcd for C₄₈H₃₄ 610.2661 [M⁺]; found 610.2661 [M⁺].

7-tert-Butyl-1,3-diphenyl-5,9-bis-(4'-fluorophenylethynyl)pyrene **4b** was obtained as a pale-yellow solid (recrystallized from hexane:CH₂Cl₂=3:1, 104 mg, 61%). M.p. 286–287°C; ¹H NMR (400 MHz, CDCl₃): $\delta_{\text{H}} = 1.68$ (s, 9H, *t*Bu), 7.13 (t, $J = 8.6$ Hz, 4H, Ar-*H*), 7.53 (t, $J = 7.5$ Hz, 2H, Ar-*H*), 7.60 (t, $J = 7.4$ Hz, 4H, Ar-*H*), 7.68 (d, $J = 7.3$ Hz, 8H, Ar-*H*), 7.96 (s, 1H, pyrene-*H*), 8.47 (s, 2H, pyrene-*H*), 8.89 (s, 2H, pyrene-*H*) ppm; ¹³C NMR (100 MHz, CDCl₃): $\delta_{\text{C}} = 32.02, 35.82, 88.02, 93.64, 110.02, 115.82, 116.04, 120.50, 121.77, 126.94, 127.67, 128.64, 129.70, 129.89, 130.44, 130.69, 133.59, 133.68, 138.44, 140.59, 149.79, 161.44$ ppm; FAB-MS: m/z calcd for C₄₈H₃₂F₂ 646.2472 [M⁺]; found 646.2472 [M⁺].

7-tert-Butyl-1,3-diphenyl-5,9-bis-(4'-methoxyphenylethynyl)pyrene **4c** was obtained as a yellow solid (recrystallized from hexane:CH₂Cl₂=4:1, 101 mg, 57%). M.p. 335–336°C; ¹H NMR (400 MHz, CDCl₃): $\delta_{\text{H}} = 1.68$ (s, 9H, *t*Bu), 3.87 (s, 6H, OMe), 6.92–6.98 (m, 4H, Ar-*H*), 7.51 (t, $J = 7.3$ Hz, 2H, Ar-*H*), 7.57–7.66 (m, 8H, Ar-*H*), 7.70 (d, $J = 7.3$ Hz, 4H, Ar-*H*), 7.94 (s, 1H, pyrene-*H*), 8.45 (s, 2H, pyrene-*H*), 8.92 (s, 2H, pyrene-*H*) ppm; ¹³C NMR (100 MHz, CDCl₃): $\delta_{\text{C}} = 31.94, 35.59, 55.33, 87.03, 94.71, 114.16, 115.47, 120.86, 121.74, 123.11, 124.39, 126.93, 127.47, 128.51, 129.02, 129.71, 130.40, 130.63, 133.14, 137.94, 140.62, 149.66, 159.79$ ppm; FAB-MS: m/z calcd for C₅₀H₃₈O₂ 670.2872 [M⁺]; found 670.2872 [M⁺].

7-tert-Butyl-1,3-diphenyl-5,9-bis-(4'-formylphenylethynyl)pyrene **4e** was obtained as an orange solid (recrystallized from hexane:CH₂Cl₂=2:1, 81 mg, 46%). M.p. 256–257°C; ¹H NMR (400 MHz, CDCl₃): $\delta_{\text{H}} = 1.70$ (s, 9H, *t*Bu), 7.55 (d, $J = 6.3$ Hz, 2H, Ar-*H*), 7.61 (t, $J = 6.8$ Hz, 4H, Ar-*H*), 7.70 (d, $J = 7.4$ Hz, 4H, Ar-*H*), 7.80 (d, $J = 7.9$ Hz, 4H, Ar-*H*), 7.90 (d, $J = 7.0$ Hz, 4H, Ar-*H*), 7.98 (s, 1H, pyrene-*H*), 8.50 (s, 2H, pyrene-*H*), 8.88 (s, 2H, pyrene-*H*), 10.03 (s, 2H, CHO) ppm; ¹³C NMR (100 MHz, CDCl₃): $\delta_{\text{C}} = 31.80, 35.53, 92.16, 93.71, 121.53, 126.51, 127.62, 128.50, 128.74, 129.37, 129.56, 129.84, 130.02, 130.34, 130.46, 131.95, 135.37, 138.77, 149.71, 191.16$ ppm; FAB-MS: m/z calcd for C₅₀H₃₄O₂ 666.2559 [M⁺]; found 666.2559

355
356
357
358 [M⁺].

359 7-*tert*-Butyl-1,3-diphenyl-5,9-bis-(4'-*N,N*-dimethylphenylethynyl)pyrene **4f** was obtained
360 as a yellow solid (recrystallized from hexane:CH₂Cl₂=4:1, 107 mg, 58%). M.p. 346–347°C; ¹H
361 NMR (400 MHz, CDCl₃): δ_H = 1.68 (s, 9H, *t*Bu), 3.03 (s, 12H, Me), 6.74 (d, *J* = 8.4 Hz, 4H,
362 Ar-*H*), 7.50 (t, *J* = 6.9 Hz, 2H, Ar-*H*), 7.59 (t, *J* = 7.7 Hz, 8H, Ar-*H*), 7.70 (d, *J* = 7.7 Hz, 4H,
363 Ar-*H*), 7.92 (s, 1H, pyrene-*H*), 8.42 (s, 2H, pyrene-*H*), 8.94 (s, 2H, pyrene-*H*) ppm; ¹³C NMR
364 (100 MHz, CDCl₃): δ_C = 32.35, 35.97, 40.43, 40.55, 73.01, 82.73, 86.82, 96.51, 108.93, 110.44,
365 112.02, 112.28, 121.78, 122.18, 123.51, 124.46, 127.45, 127.74, 128.64, 128.85, 130.02,
366 130.86, 131.04, 133.19, 133.95, 137.86, 141.16, 149.84, 150.56, 150.65 ppm; FAB-MS: *m/z*
367 calcd for C₅₂H₄₄N₂ 696.3504 [M⁺]; found 696.3504 [M⁺].
374

375 2.3. X-ray Crystallography

376 A crystal of **4c** suitable for X-ray diffraction study was obtained from CHCl₃ /hexane
377 solution, sealed in glass capillaries under argon, and mounted on a diffractometer. The
378 preliminary examination and data collection was performed using a Bruker APEX 2 CCD
379 detector system single-crystal X-ray diffractometer equipped with a sealed-tube X-ray source
380 (50 kV × 30 mA) using graphite-monochromated Mo Kα radiation. Data were corrected for
381 Lorentz and polarisation effects and for absorption [20]. The structure was solved by charge
382 flipping or direct methods algorithms and refined by full-matrix least-squares methods, on *F*²
383 [21]. All esds (except the esd in the dihedral angle between two l.s. planes) are estimated using
384 the full covariance matrix. The cell esds are taken into account individually in the estimation
385 of esds in distances, angles and torsion angles; correlations between esds in cell parameters are
386 only used when they are defined by crystal symmetry. An approximate (isotropic) treatment of
387 cell esds is used for estimating esds involving l.s. planes. The final cell constants were
388 determined through global refinement of the xyz centroids of the reflections harvested from
389 the entire data set. Structure solution and refinement were carried out using the SHELXTL-
390 PLUS software package [22]. CCDC-1547621 (**4c**) contain supplementary crystallographic
391 data for this paper. Copies of the data can be obtained, free of charge, on application to CCDC,
392 12 Union Road, Cambridge CB2 1EZ, UK [fax: 144-1223-336033 or e-mail:
393 deposit@ccdc.cam.ac.uk].
404
405
406
407
408
409
410
411
412
413

3. Results and discussion

Scheme 1

Table 1

To fulfil these requirements, we present herein a direct strategy to eliminate the problematic issues discussed above, see [Scheme 1](#), by constructing a new push-pull structure (dipolar molecules) to achieve functionalization at the active sites (1,3-positions) and K-region (5,9-positions) of pyrene based on the activity of the bromination reaction. Using 7-*tert*-butyl-1,3-diphenylpyrene (**2**) [23] as the key starting material, 7-*tert*-butyl-1,3-diphenyl-5,9-dibromopyrene **3b** was then prepared from **2** with 3.0 equiv. bromine in CH₂Cl₂ in the presence of iron-powder in high yield (up to 83%). It is worth noting that this type of reaction did not occur in the absence of iron powder and only a trace amount of **3a** was detected (entry 1). Moreover, in order to optimize and improve this practical strategy, we carried out this reaction under different conditions, and an efficient, controllable bromination strategy was established. These optimized conditions and results are summarized in [Table 1](#). Generally, the selectivity of functionalization between the K-region and *para* position of phenyl ring could be achieved by adjusting the amount of bromine and iron powder, which depends on the activity in different sites. This is the first reported example of the controllable, regioselective, and highly efficient bromination of pyrene at the K-region positions, and this highlighting methodology indeed exhibited the significance to stimulate new fundamental and theoretical studies, which is helpful to understand the mechanism of the molecular structure and photophysical properties. A set of dipolar fluorophores **4**, based on this intermediate bromopyrene **3b**, were then obtained, in considerable yields, by a Sonogashira coupling reaction ([Scheme 2](#)). The detailed synthetic procedures are described in the supporting information (ESI†); all the new compounds **3** and **4** were fully characterized by ¹H/¹³C NMR spectroscopy and high resolution mass spectrometry ([Figs. S1–15](#), ESI†). The thermal properties of **4a–f** were studied using thermogravimetric analysis (TGA) under a nitrogen atmosphere at a heating rate of 10 °C min⁻¹, as shown in [Table 2](#) and [Fig. S16](#). It can be seen that fluorophores **4** showed very high thermal stability with decomposition temperatures (*T_d*) of 356 to 527 °C and melting temperatures (*T_m*) of 256 to 352

473
474
475
476 °C. These results revealed that the fluorophores **4** showed high thermal stabilities, which
477 suggest great potential application in organic electronics applications.
478
479
480

481 482 483 484 485 486 487 488 489 490 491 492 493 494 495 496 497 498 499 500 501 502 503 504 505 506 507 508 509 510 511 512 513 514 515 516 517 518 519 520 521 522 523 524 525 526 527 528 529 530 531

After numerous attempts, a crystal suitable for single crystal X-ray diffraction of the fluorophore **4c** was cultivated from a CHCl₃/hexane solution, and the exact conformation was unambiguously established (Fig. 1a). The crystal structure of **4c** reveals that the molecule displays a more planar conformation with a tightly layered arrangement, which was attributed to the twist angles between the central pyrene (C1 > C 16) and terminal phenyl moieties at the 1,3-positions (61.09(8)°, 48.83(7)°), and the C₆ aromatic rings at the 5,9-positions (27.78(7)°, 24.65(6)°); the latter is less than previously reported between the pyrene core and substituents at the 1,3,5,9-positions [23,24]. Pairs of short $\pi\cdots\pi$ interactions were observed (3.25–3.35 Å) between the pyrene core and both C₆H₄OMe rings (shown in blue dashed lines). The intermolecular $\pi\cdots\pi$ interactions combined with weak intermolecular hydrogen bonded interactions (green dashed lines) result in sheet-like stacks (Fig. 1b).

Fig. 1.

Fig. 2.

Density functional theory (DFT) calculations (B3LYP/6-31 g*) were performed in order to gain a deeper insight into the relationship between the structures and properties. The value and contours of the highest occupied molecular orbitals (HOMOs) and the lowest unoccupied molecular orbitals (LUMOs) of **4** are provided in Table 2 and Fig. 2. As depicted in Fig. 2, the contours of the HOMOs and LUMOs of **4** present a reasonable difference. The HOMOs of **4a–e** are mainly distributed on the pyrene core, which resulted from the weak electron-donating ability of the phenyl moiety, while the HOMOs of **4f** are spread over the arylethynyl moiety and the pyrene core, which was attributed to the strong electron-donating nature of the *N,N*-dimethylamino groups. The LUMOs are mostly localized on the pyrene core and alkynyl moiety, especially for **4d**, **4e**, because of the strong electron-withdrawing ability of the -CN and -CHO moieties. The theoretical results demonstrate that the ability for intramolecular

532
533
534
535 charge transfer of **4d–f** allows them to exhibit enhanced ICT character versus **4a–c**. In other
536 words, the emission behavior is sensitive to environmental change, which impacts on the
537 separation of the HOMOs and LUMOs, particularly polarity [25].
538
539
540
541
542

543
544 **Table 2.**
545

546
547
548 **Fig. 3.**
549

550 Further investigations of the photophysical properties were carried out both in solution and
551 in the solid state based on our preliminary theoretical guidance. As depicted in Fig. 3 and Table
552 2, two sets of pronounced absorption bands were observed for fluorophores **4**, mainly centered
553 at 334–354 nm (high-energy band), and 375–395 nm (low-energy band). More specifically, the
554 high-energy band is mainly associated with the $S_2 \leftarrow S_0$ and $S_1 \leftarrow S_0$ absorption transitions of
555 the arylolethynyl and pyrene core with high molar absorption coefficients ($34481\text{--}73883\text{ cm}^{-1}\text{ M}^{-1}$).
556 The values exhibit an increasing trend following the order from **4a** to **4f**, while the molar
557 absorption coefficient of low-energy ($34066\text{--}81269\text{ cm}^{-1}\text{ M}^{-1}$) also follow this trend. Further,
558 a weak band in the high-energy absorption region (299–308 nm) can be ascribed to the $S_3 \leftarrow$
559 S_0 transitions of the phenyl and pyrene core with low molar absorption coefficients
560 ($31608\text{--}55690\text{ cm}^{-1}\text{ M}^{-1}$) [10]. This low-energy absorption band for **4** indicates that their
561 excited states possess significant charge transfer (CT) absorption associated with the ICT from
562 the 1,3-diphenyl to the 5,9-diarylolethynyl terminal substituents via the pyrene core, which is
563 also consistent with the separation of the HOMO and LUMO distributions as determined by
564 the DFT calculations.
565
566
567
568
569
570
571
572
573
574
575
576
577
578
579

580 **Fig. 4.**
581

582 Enough interest was aroused to investigate the emission properties because of their sensitive
583 molar absorption coefficients, arising from the small differences in their substituents at the para
584 position of the arylolethynyl group. For example, these six fluorophores **4** exhibit distinct
585
586
587
588
589
590

591
592
593
594
595
596
597
598
599
600
601
602
603
604
605
606
607
608
609
610
611
612
613
614
615
616
617
618
619
620
621
622
623
624
625
626
627
628
629
630
631
632
633
634
635
636
637
638
639
640
641
642
643
644
645
646
647
648
649

emission properties and solvatochromic effects between fluorophores **4a–c** and fluorophores **4d–f**. The fluorescence profiles in dilute dichloromethane solution exhibit a tunable emission wavelength in the range 426–520 nm. There was no observable bathochromic shift trend (< 5 nm) between **4a–c**, while **4d–f** exhibited a distinct bathochromic shift (26–94 nm) compared with the former. The emission maxima of this set of fluorophores follow the order $4a \approx 4b \approx 4c < 4d < 4e < 4f$ (Fig. 4a). To further verify the tunable wide visible emission of this system, their emission properties in the solid state were also investigated (Fig. 4b). The emissions of **4a–c** are drastically red-shifted by more than 78 nm (139 nm for **4a**, 78 nm for **4b** and 80 nm for **4c**), these distinctions in solution and in the solid state are mainly due to enhanced electronic coupling with the restriction of the intramolecular rotation and the $\pi \cdots \pi$ interaction between the phenyl rings and the pyrene core in the solid state, because the planar structures tend to form dimers. On the other hand, the emissions of **4d–f** present minor red- or blue-shifts compared with those in CH_2Cl_2 solution (red-shift 22 nm for **4d**, 17 nm for **4e** and blue-shift 7 nm for **4f**), presumably, which is ascribed to the bulky substituents at the para position of the arylolethynyl group, which could suppress the aggregation in the solid state and tune the energy gap via the effect of the conformation of the electronic structures [26]. By comparison, this type of dipolar molecules exhibited more tunable and sensitive emission properties than do the 1,3,5,9-tetraarylpyrenes and 1,3,6,8-tetraalkynylpyrenes both in solution and in the solid state [24,27], which was attributed to the enhancement of the intramolecular charge-transfer for the “push-pull-type” systems.

Fig. 5.

In order to study the solvatochromism of these systems, solvents of various polarities, namely cyclohexane (CHX), tetrahydrofuran (THF), dichloromethane (DCM), acetonitrile (ACN), and dimethylformamide (DMF), were selected, and the absorption and emission spectra were recorded (Fig. 5a, and Figs. S17–18, ESI†). The absorption spectra of **4** manifest none or minimum solvent dependence. On the contrary, the solvatochromism could also be divided into two groups. For **4a–c**, there was little effect on the λ_{max} for the emission profiles from CHX to DMF (7 nm for **4a**, 7 nm for **4b** and 11 nm for **4c**). In sharp contrast, the emission

650
651
652
653 profiles of **4d–f** exhibited a significant red-shift as large as 134 nm for **4f**. Take **4f** as example,
654 the fluorophore **4f** exhibited distinct color change from deep blue in cyclohexane to green,
655 yellow, or even orange-red in DMF, which was observed under a UV light (365 nm), as shown
656 in Fig. 5b. This further indicates that fluorophores **4** are favorable, tunable fluorescent materials.
657
658 This phenomenon of solvatochromism was further confirmed by the relationship between the
659 Stokes shifts in various solvents and the Lippert equation [28], Lippert-Mataga plot showed
660 the linear correlation together with an increasing slope from **4a** to **4f**, meaning the
661 intramolecular excited state with an increasing dipolar moment than the ground state due to the
662 substantial charge redistribution (Fig. S19). The value of the slope for **4f** (16681) is far larger
663 than that for **4a** (1046). Moreover, compared with the other five compounds, the absorption
664 spectra of fluorophore **4f** presents obvious red-shift with increase of solvent polarity (λ_{max} : 371
665 nm in cyclohexane \rightarrow 382 nm in DMF), so the twisted intramolecular charge transfer (TICT)
666 might plays an important role in the solution state [29]. In nonpolar solvent, the more planar
667 conformation of **4** is stabilized by electronic conjugation, which results in a sharp fluorescence
668 spectrum on its locally excited (LE) state. The trend for intramolecular twisting in the polar
669 solvent, however, transforms **4** from the LE state to the TICT state. The twisted conformation
670 of **4** is stabilized due to the solvating effect of the polar solvent. Furthermore, this generates a
671 smaller energy gap, hence bathochromically shifting its PL spectrum, especially for compounds
672 **4d–f**, due to the substituents at the para position of the arylethynyl group. This is now the
673 highest tunable system bearing of 1,3-diphenyl-5,9-di-substituents at pyrene. As a control,
674 more distinct charge separations and higher tunability were observed versus the 1,3-diphenyl-
675 6,8-di-substituents pyrene systems [10b].
676
677
678
679
680
681
682
683
684
685
686
687
688
689
690
691

692 The oxidative electrochemical behavior of fluorophores **4** was investigated by cyclic
693 voltammetry (CV) using ferrocene as the internal standard. All of the fluorophores **4** displayed
694 irreversible oxidation processes with distinct positive potentials ranging from 0.73 to 1.22 V in
695 CH_2Cl_2 solution, as shown in Fig. S20, and Table 2. This can be associated with the terminal
696 nature of the functional groups. The HOMOs of fluorophores **4a–f** were estimated to be -5.55 ,
697 -5.57 eV, -5.52 eV, -5.64 eV, -5.61 eV, -5.15 eV, respectively. The trend in the values is in
698 good agreement with the DFT calculation results. The LUMOs were also evaluated from CVs
699 and the UV-vis absorption to be in the range -1.90 eV to -2.41 eV. These results suggest that
700
701
702
703
704
705
706
707
708

709
710
711 these dipolar molecules possess good hole- and electron-transporting properties [30].
712
713
714

715 716 **4. Conclusion** 717

718
719 In summary, we present a facile, and controllable regioselective strategy for the
720 functionalization of pyrene both at the active sites (1,3-positions) by Suzuki cross-coupling
721 reaction and K-region (5,9-positions) by Sonogashira coupling reaction based on the
722 bromination reaction stepwise. Depending on the electron-donating/withdrawing groups with
723 an extended π -conjugation, the resulting six dipolar molecules, namely 1,3-diphenyl-5,9-
724 diarylethynyl)pyrenes, exhibit thermal stability (> 256 °C) and wide-range color tuning.
725 Especially for compound **4f**, a significant solvatochromism effect with a large red-shift (134
726 nm) were observed from non-polar solvent (cyclohexane) to polar solvent (DMF). The
727 combined experimental and computational results provide an increasing understanding of the
728 emission mechanism for introducing substitution at the K-region of pyrene. This work opens
729 up new avenues to explore strategy to functionalize pyrene and to greatly expand the scope for
730 developing highly efficient pyrene-based photoelectric materials.
731
732
733
734
735
736
737
738
739
740
741

742 743 **Acknowledgments** 744

745
746 This work was performed under the Cooperative Research Program of “Network Joint
747 Research Center for Materials and Devices (Institute for Materials Chemistry and Engineering,
748 Kyushu University)”. We would like to thank the National Science Foundation of China (No.
749 21602014), Fund Program for the Scientific Activities of Selected Returned Overseas
750 Professionals of Beijing, the OTEC at Saga University and the International Cooperation
751 Projects of Guizhou Province (No. 20137002), the Royal Society of Chemistry for financial
752 support, and the EPSRC for an overseas travel grant to C.R.
753
754
755
756
757
758
759
760

761 **References** 762 763 764 765 766 767

- 768
769
770
771 [1] (a) Wu KC, Ku PJ, Lin CS, Shih HT, Wu FI, et al. The photophysical properties of
772 dipyrenylbenzenes and their application as exceedingly efficient blue emitters for
773 electroluminescent devices. *Adv. Funct Mater* 2008;18:67–75; (b) Wong WY, Ho CL, Gao
774 ZQ, Mi BX, Chen CH, et al. Multifunctional iridium complexes based on carbazole
775 modules as highly efficient electrophosphors. *Angew Chem Int Ed* 2006;45:7800–3.
776
777
778
779 [2] Liu ZC, Yin LJ, Ning H, Yang ZY, Tong LM, Ning CZ. Dynamical color-controllable
780 lasing with extremely wide tuning range from red to green in a single alloy nanowire using
781 nanoscale manipulation. *Nano Lett* 2013;13:4945–50.
782
783
784
785 [3] (a) Lin YZ, Zhao FW, He Q, Wu LJ, Parker TC, et al. High-performance electron acceptor
786 with thienyl side chains for organic photovoltaics. *J Am Chem Soc* 2016;138:4955–61; (b)
787 Liang XY, Bai S, Wang X, Dai XL, Gao F, et al. Colloidal metal oxide nanocrystals as
788 charge transporting layers for solution-processed light-emitting diodes and solar cells.
789 *Chem Soc Rev* 2017;46:1730–59; (c) Mei J, Leung NLC, Kwok RTK, Lam JWY, Tang
790 BZ. Aggregation-induced emission: together we shine, united we soar! *Chem Rev*
791 2015;115:11718–940.
792
793
794
795
796
797 [4] (a) Winkler, JR, Gray HB. Long-range electron tunneling. *J Am Chem Soc*
798 2014;136:2930–9; (b) Bilici A, Doğan F, Yildirim M, Kaya I. Tunable multicolor emission
799 in oligo (4-hydroxyquinoline). *J Phys Chem C* 2012;116:19934–40.
800
801
802 [5] Milián-Medina B, Gierschner JJ. "Though it be but little, it is fierce": excited state
803 engineering of conjugated organic materials by fluorination. *Phys Chem Lett*
804 2017;8:91–101.
805
806
807 [6] (a) Merz J, Fink J, Friedrich A, Krummenacher I, Mamari HA, et al. Pyrene molecular
808 orbital shuffle—controlling excited state and redox properties by changing the nature of
809 the frontier orbitals. *Chem -Eur J* 2017;23:13164–80; (b) Li SS, Jiang KJ, Yu CC, Huang
810 JH, Yang LM, Song YL. A 2,7-pyrene-based dye for solar cell application. *New J Chem*
811 2014;38:4404–8; (c) Kurata R, Ito A, Gon M, Tanaka K, Chujo Y. Diarylamino- and
812 diarylboryl-substituted donor–acceptor pyrene derivatives: influence of substitution pattern
813 on their photophysical properties. *J Org Chem* 2017;82:5111–21.
814
815
816
817
818
819
820
821
822
823
824
825
826

- 827
828
829
830 [7] Yang W, Pan CY, Luo MD, Zhang HB. Fluorescent mannose-functionalized hyperbranched
831 poly (amido amine) s: synthesis and interaction with E. coli. *Biomacromolecules*
832 2010;11:1840–6.
833
834
835 [8] Wang J, Tang S, Sandström A, Edman L. Combining an Ionic Transition Metal Complex
836 with a Conjugated Polymer for Wide-Range Voltage-Controlled Light-Emission Color.
837 *ACS Appl Mater Interfaces* 2015;7:2784–9.
838
839
840 [9] (a) Mizoshita N, Goto Y, Maegawa Y, Tani T, Inagaki S. Tetraphenylpyrene-bridged
841 periodic mesostructured organosilica films with efficient visible-light emission. *Chem*
842 *Mater* 2010;22:2548–54; (b) Zhang ZY, Wu YS, Tang KC, Chen CL, Ho JW, et al. Excited-
843 state conformational/electronic responses of saddle-shaped N,N'-disubstituted-
844 dihydrodibenzo[a,c]phenazines: wide-tuning emission from red to deep blue and white
845 light combination. *J Am Chem Soc* 2015;137:8509–20.
846
847
848
849
850
851 [10] Crawford AG, Dwyer AD, Liu ZQ, Steffen A, Beeby A, et al. Experimental and theoretical
852 studies of the photophysical properties of 2-and 2, 7-functionalized pyrene derivatives. *J*
853 *Am Chem Soc* 2011;133:13349–62.
854
855
856 [11] Hu JY, Era M, Elsegood MRJ, Yamato T. Synthesis and photophysical properties of
857 pyrene-based light-emitting monomers: highly pure-blue-fluorescent, cruciform-shaped
858 architectures. *Eur J Org Chem* 2010;72–9.
859
860
861 [12] (a) Zöphel L, Beckmann D, Enkelmann V, Chercka D, Rieger R, Müllen K. Asymmetric
862 pyrene derivatives for organic field-effect transistors. *Chem Commun* 2011;47:6960–2;
863 (b). Zöphel L, Enkelmann V, Müllen K. Tuning the HOMO-LUMO gap of pyrene
864 effectively via donor-acceptor substitution: positions 4,5 versus 9,10. *Org Lett*
865 2013;15:804–7; (c) Keller SN, Veltri NL, Sutherland TC. Tuning light absorption in
866 pyrene: synthesis and substitution effects of regioisomeric donor-acceptor chromophores.
867 *Org Lett* 2013;15:4798–801; (d) Keller SN, Bromby AD, Sutherland TC. Optical effect of
868 varying acceptors in pyrene donor–acceptor–donor chromophores. *Eur J Org Chem*
869 2017;3980–5.
870
871
872
873
874
875
876
877
878 [13] (a) Figueira-Duarte TM, Müllen K. Pyrene-based materials for organic electronics. *Chem*
879 *Rev* 2011;111:7260–314; (b) Mateo-Alonso A. Pyrene-fused pyrazaacenes: from small
880 molecules to nanoribbons. *Chem Soc Rev* 2014;43:6311–24; (c) Casas-Solvas JM,
881
882
883
884
885

- 886
887
888
889 Howgego JD, Davis AP. Synthesis of substituted pyrenes by indirect methods. *Org Biomol*
890 *Chem* 2014;12:212–32; (d) Feng X, Hu JY, Redshaw C, Yamato T. Functionalization of
891 pyrene to prepare luminescent materials—typical examples of synthetic methodology.
892 *Chem -Eur J* 2016;22:11898–916; (e) Feng X, Tomiyasu H, Hu JY, Wei XF, Redshaw C,
893 et al. Regioselective substitution at the 1, 3-and 6, 8-positions of pyrene for the construction
894 of small dipolar molecules. *J Org Chem* 2015;80:10973–8; (f) Wang CZ, Ichiyanagi H,
895 Sakaguchi K, Feng X, Elsegood MRJ, et al. Pyrene-based approach to tune emission color
896 from blue to yellow. *J Org Chem* 2017;82:7176–82.
- [14] Hu J, Zhang D, Harris FW. Ruthenium(III) chloride catalyzed oxidation of pyrene and
903 2,7-disubstitued pyrenes: an efficient, one-step synthesis of pyrene-4,5-diones and pyrene-
904 4,5,9,10-tetraones. *J Org Chem* 2005;70:707–8.
- [15] Yamato T, Fujimoto M, Miyazawa A, Matsuo K. Selective preparation of polycyclic
909 aromatic hydrocarbons. Part 5. Bromination of 2,7-di-tert-butylpyrene and conversion into
910 pyrenoquinones and their pyrenoquinhydrones. *J Chem Soc Perkin Trans* 1997;1201–7.
- [16] Mikroyannidis JA, Stylianakis MM, Roy MS, Suresh P, Sharma GD, Synthesis,
914 photophysics of two new perylene bisimides and their photovoltaic performances in quasi
915 solid state dye sensitized solar cells. *J Power Sources* 2009;194:1171–9.
- [17] Miyazawa A, Tsuge A, Yamato T, Tashiro M. Synthesis of 4, 5-dimethyl-, 4, 5, 9-
920 trimethyl-, and 4, 5, 9, 10-tetramethylpyrene. *J Org Chem* 1991;56:4312–4.
- [18] (a) Eliseeva MN, Scott LT. Pushing the Ir-catalyzed C–H polyborylation of aromatic
923 compounds to maximum capacity by exploiting reversibility. *J Am Chem Soc*
924 2012;134:15169–72; (b) Liu ZQ, Wang YY, Chen, Y, Liu J, Fang Q, et al. Ir-catalyzed
925 direct borylation at the 4-position of pyrene. *J Org Chem* 2012;77:7124–8; (c) Ji L,
926 Fucke K, Bose SK, Marder TB. Iridium-catalyzed borylation of pyrene: irreversibility
927 and the influence of ligand on selectivity. *J Org Chem* 2015;80:661–5.
- [19] Feng X, Hu JY, Tomiyasu H, Tao Z, Redshaw C, et al. Iron(III) bromide catalyzed
934 bromination of 2-tert-butylpyrene and corresponding position-dependent aryl-
935 functionalized pyrene derivatives. *RSC Adv* 2015;5:8835–48.
- [20] APEX 2 & SAINT (2012), software for CCD diffractometers. Bruker AXS Inc.,
939 Madison, USA.
- 940
941
942
943
944

- 945
946
947
948 [21] (a) Sheldrick GM. A short history of SHELX. *Acta Cryst.* 2008;A64:112–22; (b)
949 Sheldrick GM *Acta Cryst.* SHELXT-Integrated space-group and crystal-structure
950 determination. 2015;A71:3–8; (c) Sheldrick GM. *Acta Cryst.* Crystal structure
951 refinement with SHELXL. 2015;C71:3–8.
952
953
954
955 [22] Westrip, SP. publCIF: software for editing, validating and formatting crystallographic
956 information files. *J. Appl Cryst* 2000;43:920–5.
957
958 [23] Feng X, Hu JY, Yi L, Seto N, Tao Z, et al. Pyrene-based Y-shaped solid - state blue
959 emitters: synthesis, characterization, and photoluminescence. *Chem –Asian J*
960 2012;7:2854–63.
961
962
963 [24] Feng X, Hu JY, Iwanaga F, Seto N, Redshaw C, et al. Blue-emitting butterfly-shaped 1,
964 3, 5, 9-tetraarylpyrenes: Synthesis, crystal structures, and photophysical properties. *Org*
965 *Lett* 2013;15:1318–21.
966
967
968 [25] Sasaki, S, Drummen G, Konishi G. Recent advances in twisted intramolecular charge
969 transfer (TICT) fluorescence and related phenomena in materials chemistry. *J Mater Chem*
970 *C* 2016;4:2731–43.
971
972
973 [26] Xu L, Zhang QC. Recent progress on intramolecular charge-transfer Compounds as
974 photoelectric active materials. *Sci China Mater* 2017;60:1093–101.
975
976
977 [27] (a) Oh JW, Lee YO, Kim TH, Ko KC, Lee JY, et al. Enhancement of electrogenerated
978 chemiluminescence and radical stability by peripheral multidonors on alkynylpyrene
979 derivatives. *Angew Chem Int Ed* 2009;48:2522–4; (b) Kim HM, Lee YO, Lim CS, Kim JS,
980 Cho BR. Two-photon absorption properties of alkynyl-conjugated pyrene derivatives. *J*
981 *Org Chem* 2008;73:5127–30; (c) Lee YO, Pradhan T, Yoo S, Kim TH, Kim J, Kim JS.
982 Enhanced electrogenerated chemiluminescence of phenylethynylpyrene derivatives: use of
983 weakly electron-donating group as a substituent. *J Org Chem* 2012;77:11007–13.
984
985
986 [28] (a) Lippert V. E. Z. The solvent effect on the spectral shift. *Naturforsch A: Phys Sci*
987 1955;10:541–5; (b) Mataga N, Kaifu Y, Koizumi M. Solvent effects upon fluorescence
988 spectra and the dipolemoments of excited molecules. *Bull Chem Soc Jpn* 1956;29:465–70.
989
990
991 [29] (a) Fang HH, Chen QD, Yang J, Xia H, Gao BR, et al. Two-photon pumped amplified
992 spontaneous emission from cyano-substituted oligo (p-phenylenevinylene) crystals with
993 aggregation-induced emission enhancement. *J Phys Chem C* 2010;114:11958–61; (b) Yan
994
995
996
997
998
999
1000
1001
1002
1003

1004
1005
1006
1007 ZQ, Yang ZY, Wang H, Li AW, Wang LP, Yang H, Gao BR. Study of aggregation induced
1008 emission of cyano-substituted oligo (p-phenylenevinylene) by femtosecond time resolved
1009 fluorescence. *Spectrochim Acta A: Mol Biomol Spectr* 2011;78:1640–5.
1010
1011

1012 [30] (a) Zhang Q, Li B, Huang S, Nomura H, Tanaka H, Adachi C. Efficient blue organic
1013 light-emitting diodes employing thermally activated delayed fluorescence. *Nat*
1014 *Photonics* 2014;8:326–32; (b) Reddy SS, Sree VG, Gunasekar K, Cho W, Gal Y-S, et
1015 al. Highly efficient bipolar deep-blue fluorescent emitters for solution-processed non-
1016 doped organic light-emitting diodes based on 9,9-dimethyl-9,10-
1017 dihydroacridine/phenanthroimidazole derivatives. *Adv Optical Mater* 2016;4:1236–46.
1018
1019
1020
1021
1022
1023
1024
1025
1026
1027
1028
1029
1030
1031
1032
1033
1034
1035
1036
1037
1038
1039
1040
1041
1042
1043
1044
1045
1046
1047
1048
1049
1050
1051
1052
1053
1054
1055
1056
1057
1058
1059
1060
1061
1062

List of Scheme and Figure Captions

Scheme 1. Synthetic route of precursor molecules **3**.

Scheme 2. Synthetic route of dipolar molecules **4**.

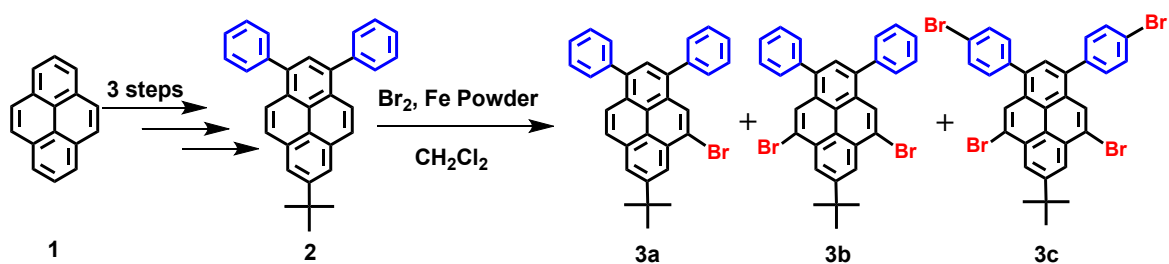
Fig. 1. (a) The crystal structure of fluorophore **4c**; (b) the principal intermolecular packing interactions.

Fig. 2. Frontier-molecular-orbital distributions and energy levels diagram of **4a–4f** by DFT calculations.

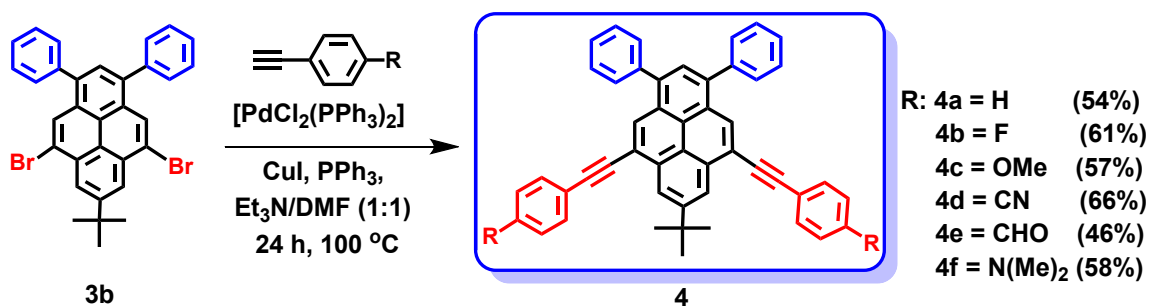
Fig. 3. UV–vis absorption spectra of compounds **4** recorded in dichloromethane solutions at $\sim 10^{-5}$ M at 25 °C.

Fig. 4. Emission spectra of fluorophores **4** in CH_2Cl_2 solution (a) and in the solid state (b).

Fig. 5. (a) Emission spectra of **4f** in solvents with varying polarity; (b) color of **4f** in different solvents under 365 nm UV illumination.



Scheme 1. Synthetic route of precursor molecules **3**.



Scheme 2. Synthetic route of dipolar molecules 4.

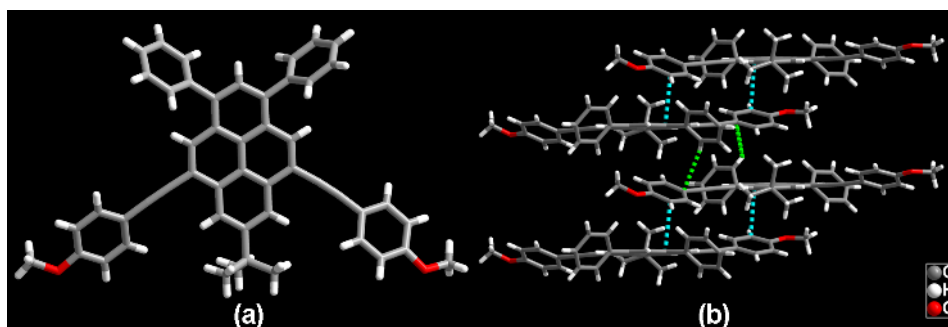


Fig. 1. (a) The crystal structure of fluorophore 4c; (b) the principal intermolecular packing interactions.

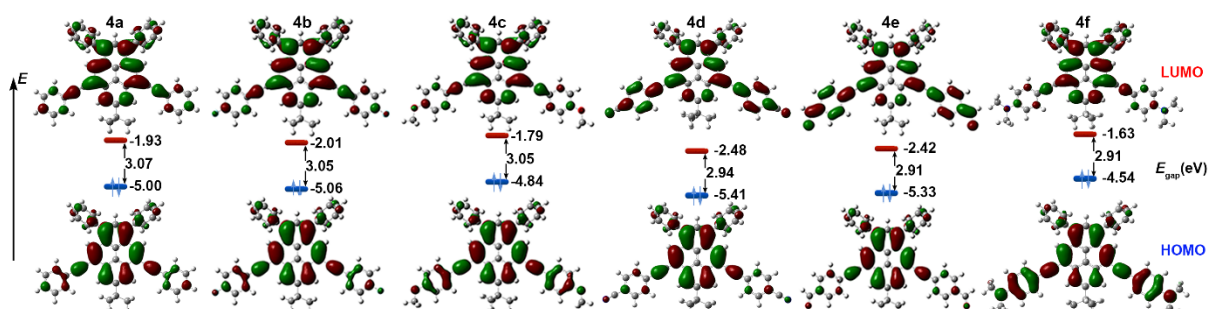


Fig. 2. Frontier-molecular-orbital distributions and energy levels diagram of 4a-f by DFT calculations.

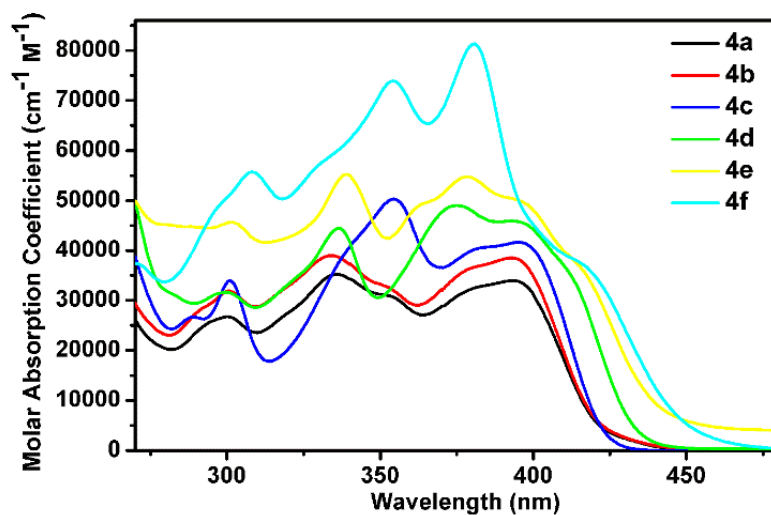


Fig. 3. UV-vis absorption spectra of compounds **4** recorded in dichloromethane solutions at $\sim 10^{-5}$ M at 25 °C.

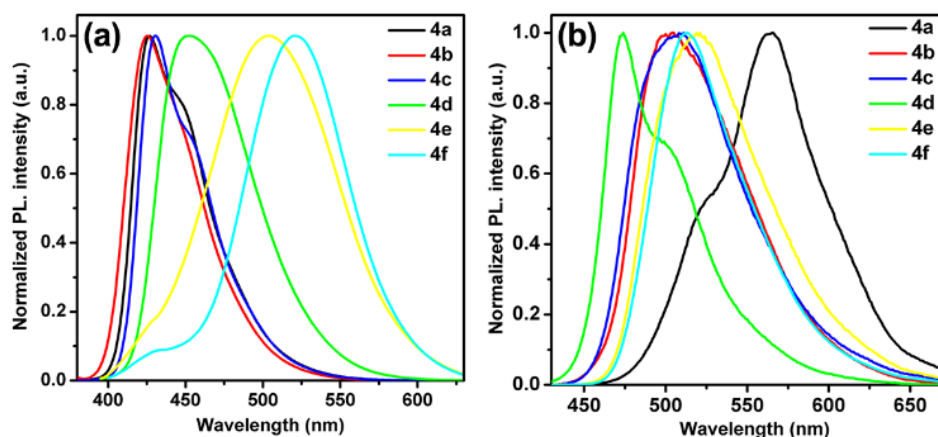


Fig. 4. Emission spectra of fluorophores **4** in CH_2Cl_2 solution (a) and in the solid state (b).

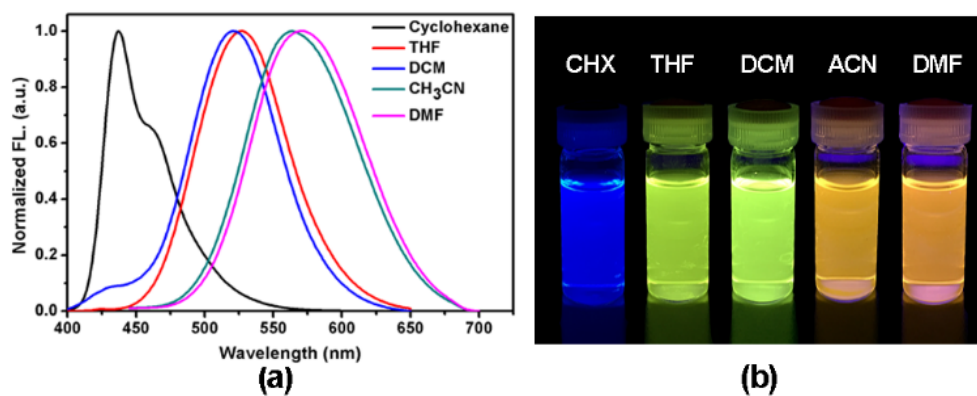


Fig. 5. (a) Emission spectra of **4f** in solvents with varying polarity; (b) color of **4f** in different solvents under 365 nm UV illumination.

Tables

Table 1 Optimization of reaction conditions to precursors **3**.

Entry	Substrate 1 (equiv)	Br ₂ (equiv)	Fe (equiv)	Products [%] ^a
1	1.0	1.5	--	3a [<5] ^b
2	1.0	1.5	1.5	3a [65]
3	1.0	3.0	3.0	3b [83]
4	1.0	6.0	6.0	3c [71]

^a The isolated yields are shown in bracket.

^b Yield was determined by ¹H NMR analysis.

Table 2. The physical properties of compounds of type **4a–f**.

R	λ_{abs} (nm) sol ^a [ϵ (M ⁻¹ cm ⁻¹ L)]	λ_{em} (nm) sol ^a /film ^b	T_{d} (°C) ^c	HOMO (eV) ^d	LUMO (eV) ^d	E_{g} (eV) ^d	HOMO (eV) ^e	LUMO (eV) ^f	E_{g} (eV) ^g	Φ_{FL} (%) sol ^a /film ^b
4a	335 (34481), 392 (34066)	427/566	525	-5.00	-1.93	3.07	-5.55	-2.39	2.78	89/9
4b	334 (38933), 393 (38486)	426/504	356	-5.06	-2.01	3.05	-5.57	-2.41	2.77	94/7
4c	354 (51366), 395 (42182)	431/511	477	-4.84	-1.79	3.05	-5.52	-2.38	2.87	98/6
4d	336 (44478), 375 (49021)	452/474	527	-5.41	-2.47	2.94	-5.64	-2.33	2.78	95/23
4e	339 (55292), 378 (54779)	504/521	356	-5.33	-2.42	2.91	-5.61	-2.33	2.58	71/4
4f	354 (73883), 381 (81269)	520/513	460	-4.54	-1.63	2.91	-5.15	-1.90	2.64	54/3

^a Measured in dichloromethane at room temperature. ^b As a thin film. ^c Obtained from TGA measurements. ^d DFT/B3LYP/6-31G* using Gaussian. ^e Measured from the oxidation potential in CH₂Cl₂ solution by cyclic voltammetry. ^f Calculated from HOMO + E_{g} . ^g Estimated from the absorption edge of UV-Vis spectra.

Pyrene-based color-tunable dipolar molecules: synthesis, characterization and optical properties

Chuan-Zeng Wang ^a, Xing Feng ^{b,*}, Zannatul Kowser ^c, Chong Wu ^a, Thamina Akther ^a, Mark R.J. Elsegood ^d, Carl Redshaw ^e, Takehiko Yamato ^{a,*}

^a Department of Applied Chemistry, Faculty of Science and Engineering, Saga University, Honjo-machi 1, Saga 840-8502 Japan.

^b Faculty of Material and Energy Engineering, Guangdong University of Technology, Guangzhou 510006, China

^c International University of Business Agriculture and Technology, Dhaka, Bangladesh

^d Chemistry Department, Loughborough University, Loughborough, LE11 3TU, UK

^e Department of Chemistry, School of Mathematics and Physical Sciences, The University of Hull, Cottingham Road, Hull, Yorkshire HU6 7RX, UK

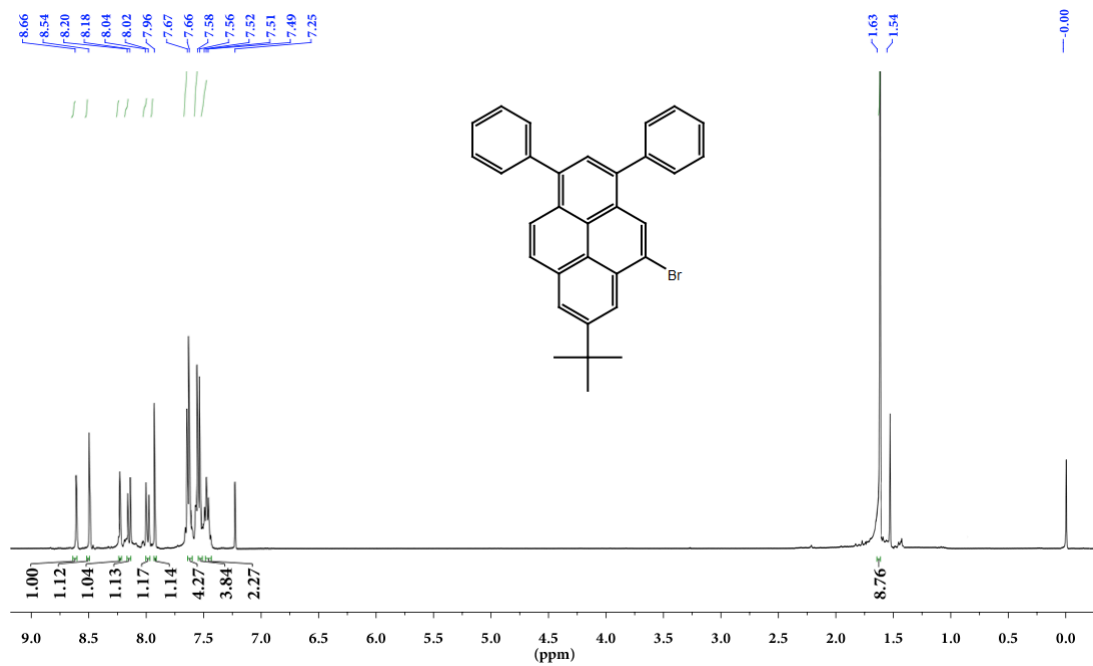


Figure S1 $^1\text{H-NMR}$ spectrum of **3a** (400 MHz, 293 K, CDCl_3).

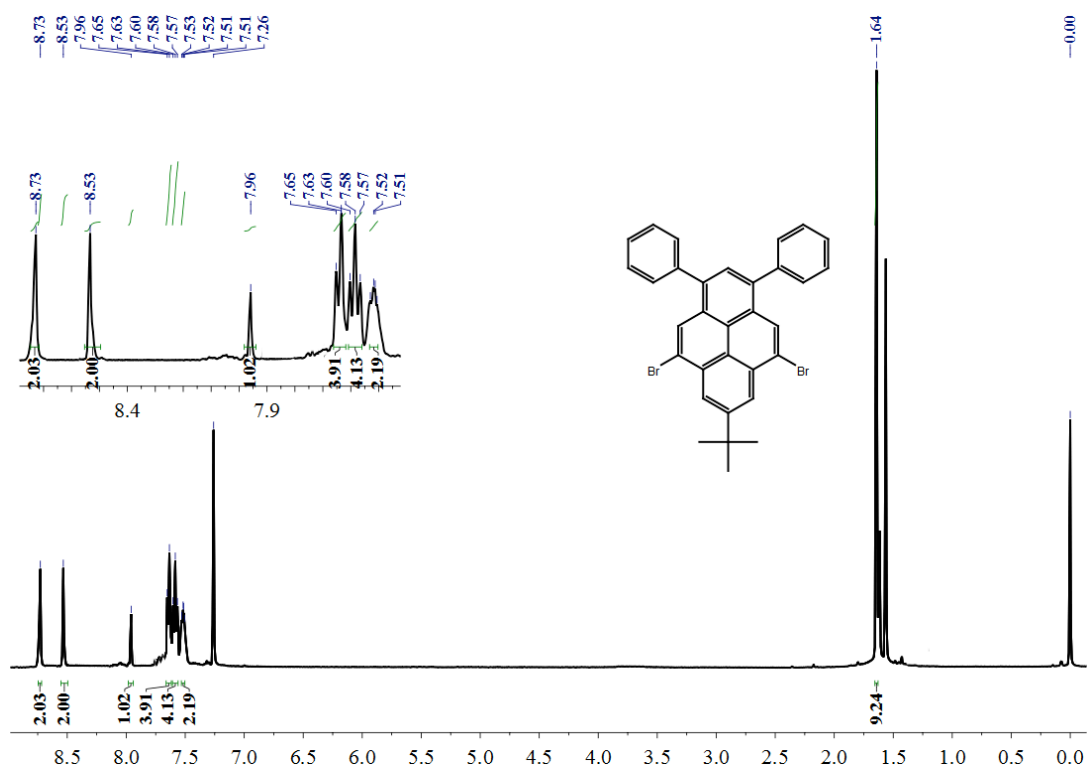


Figure S2 $^1\text{H-NMR}$ spectrum of **3b** (400 MHz, 293 K, CDCl_3).

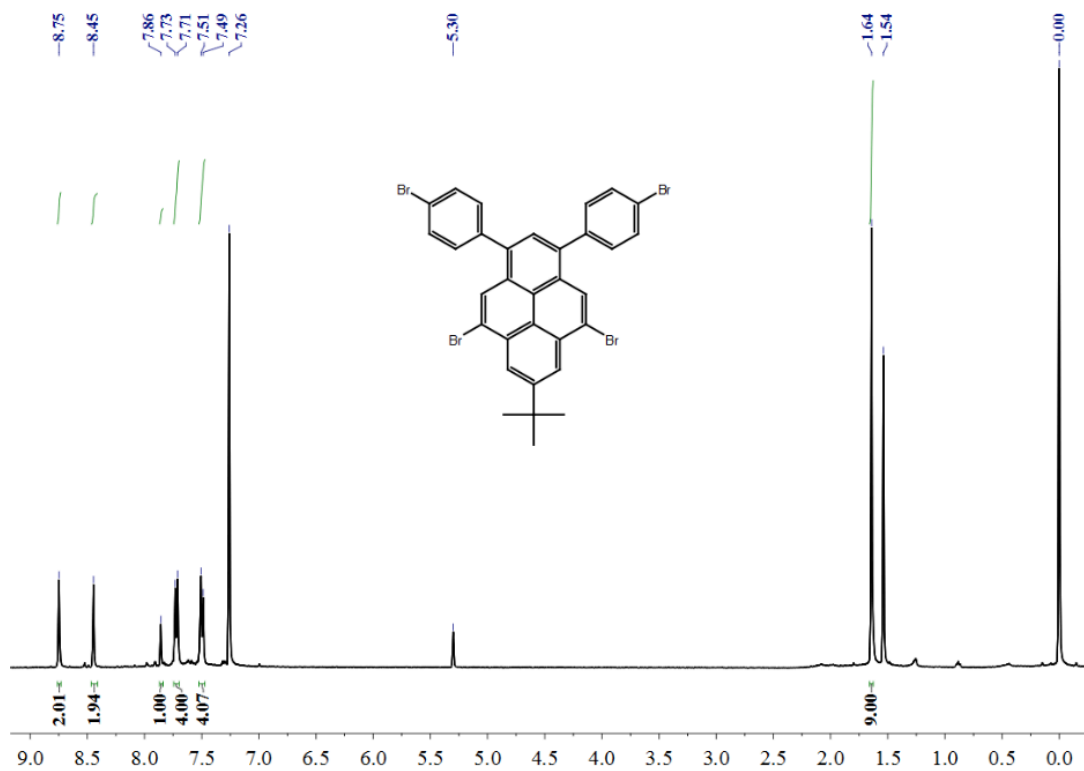


Figure S3 $^1\text{H-NMR}$ spectrum of **3c** (400 MHz, 293 K, CDCl_3).

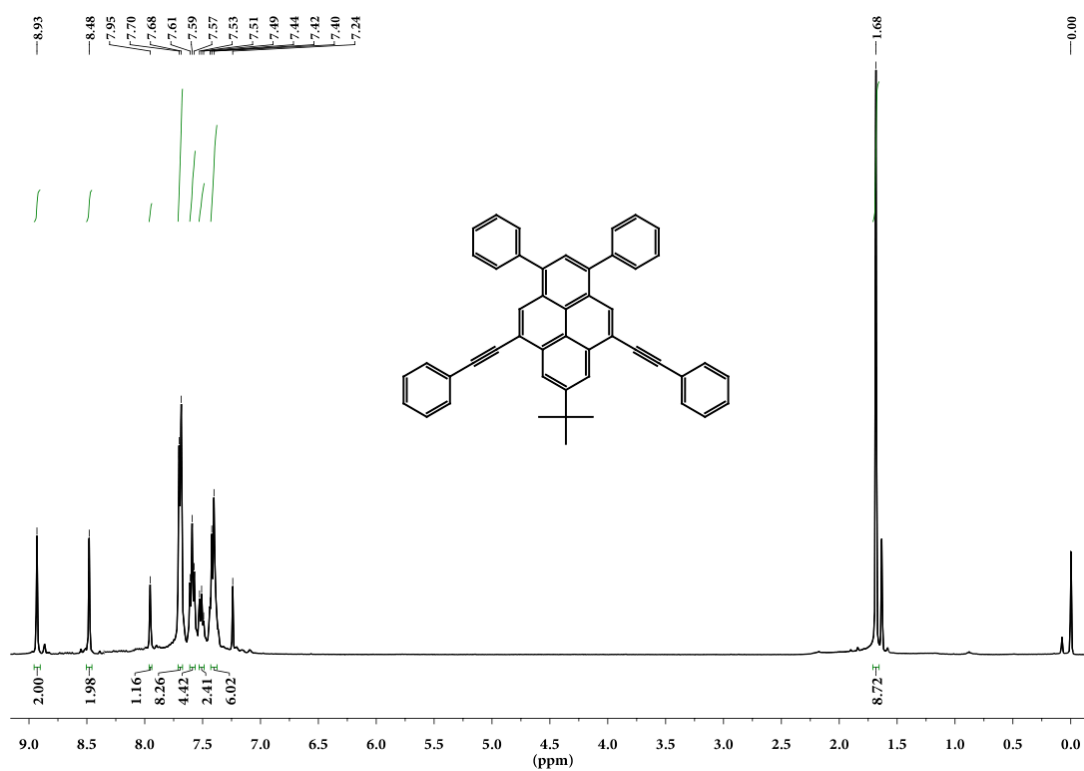


Figure S4 $^1\text{H-NMR}$ spectrum of **4a** (400 MHz, 293 K, CDCl_3).

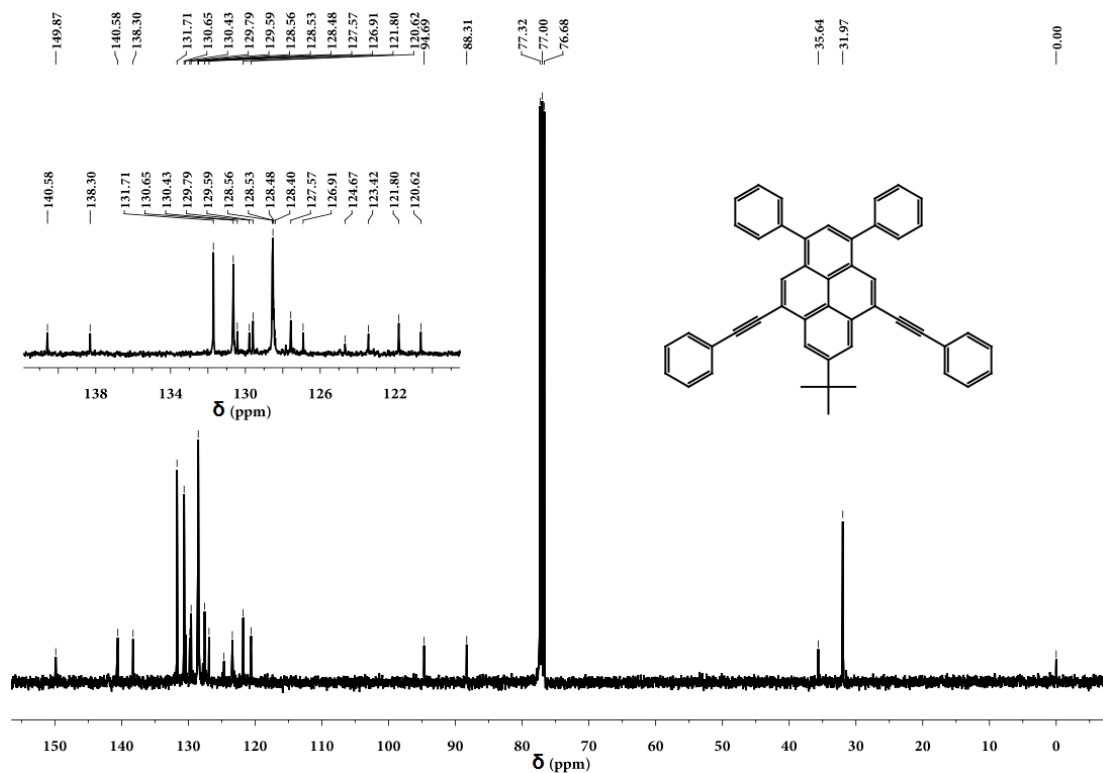


Figure S5 ^{13}C NMR spectrum of **4a** (100 MHz, 293 K, CDCl_3).

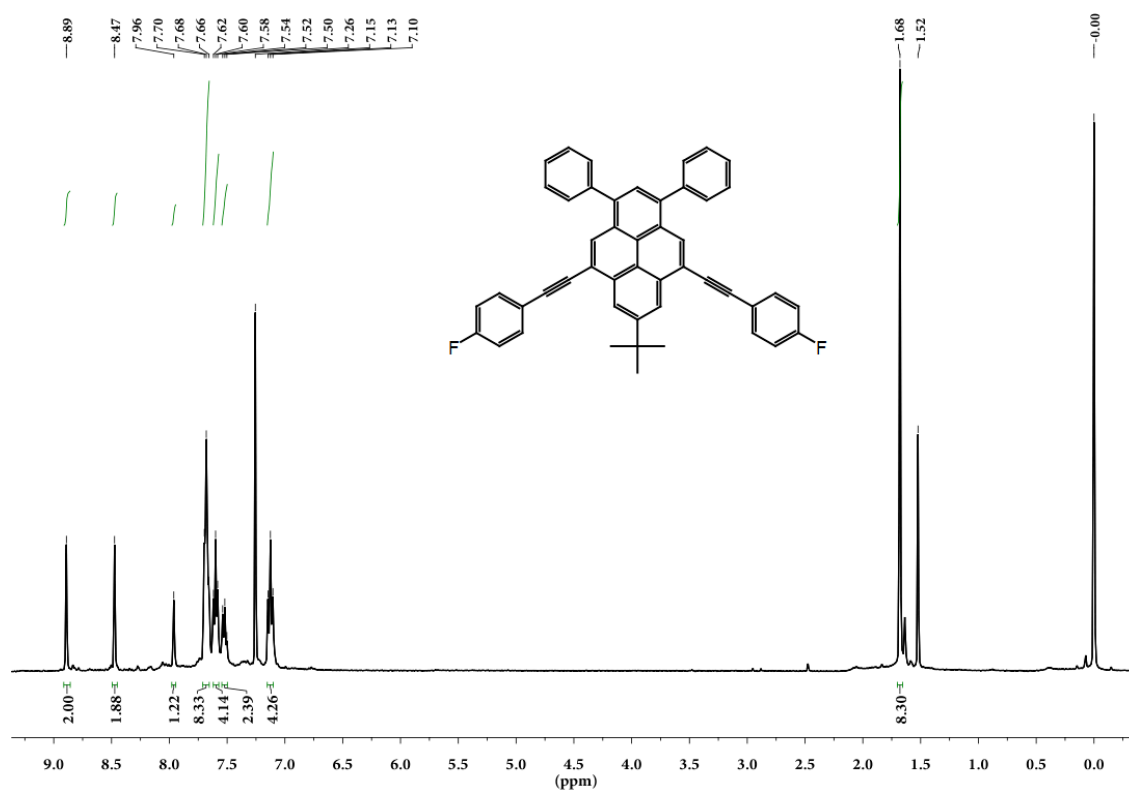


Figure S6 ^1H -NMR spectrum of **4b** (400 MHz, 293 K, CDCl_3).

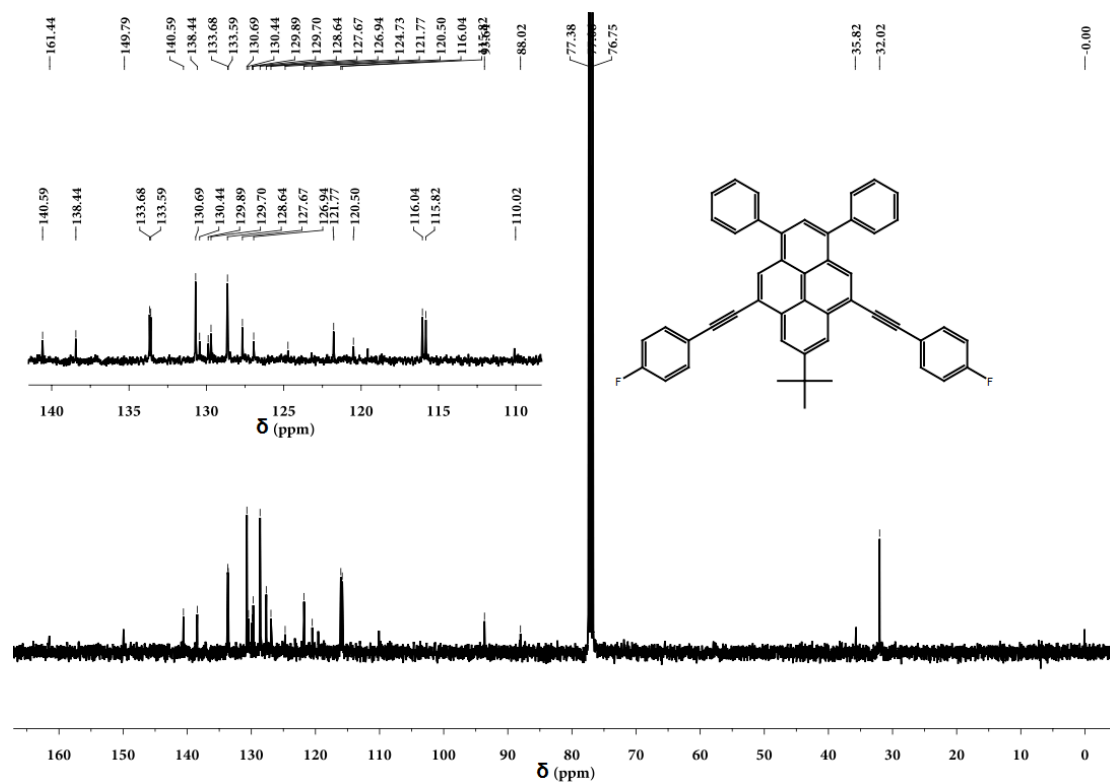


Figure S7 ^{13}C NMR spectrum of **4b** (100 MHz, 293 K, CDCl_3).

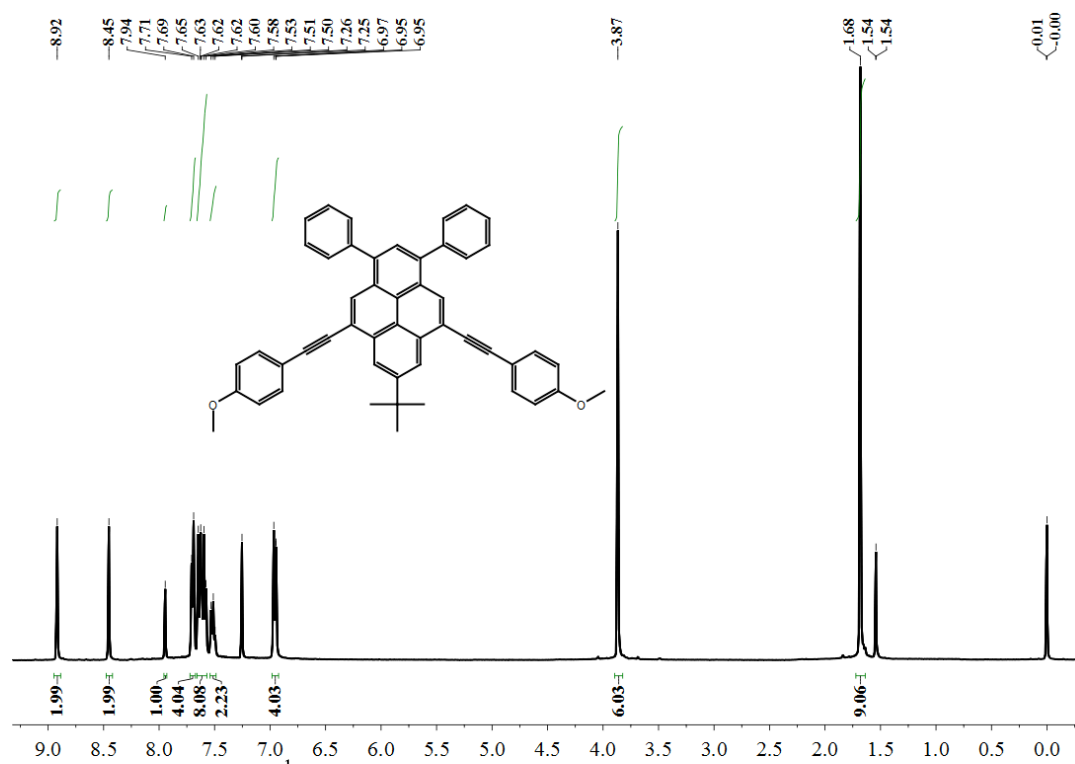
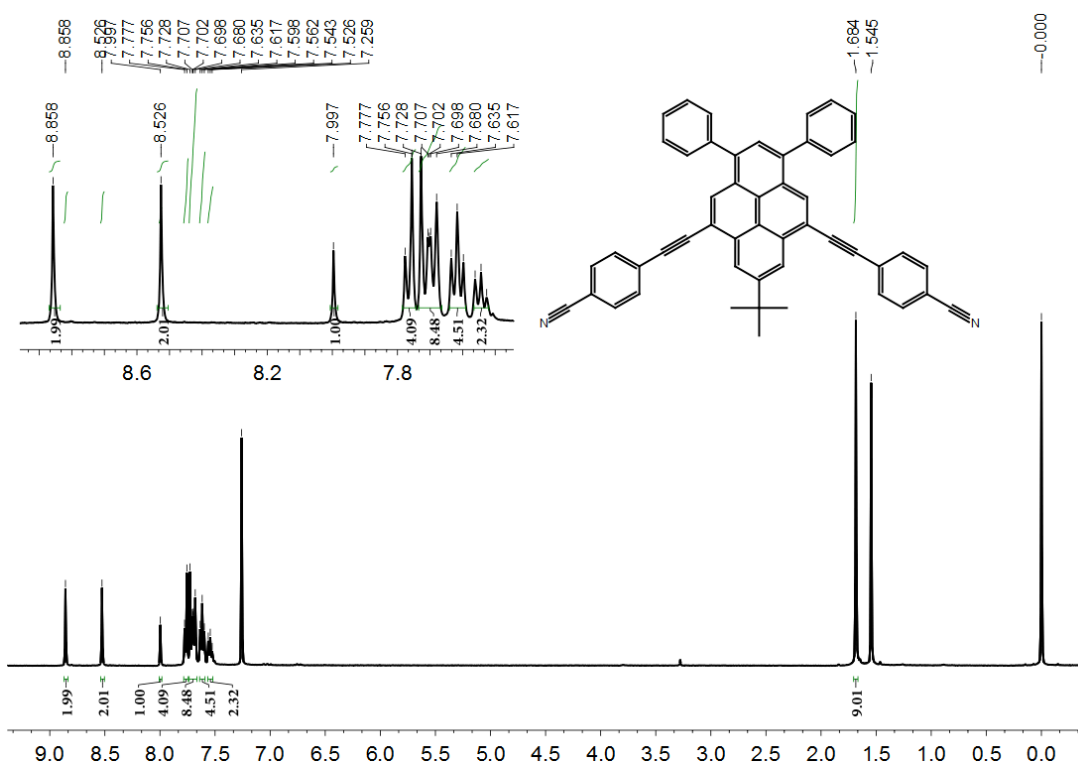
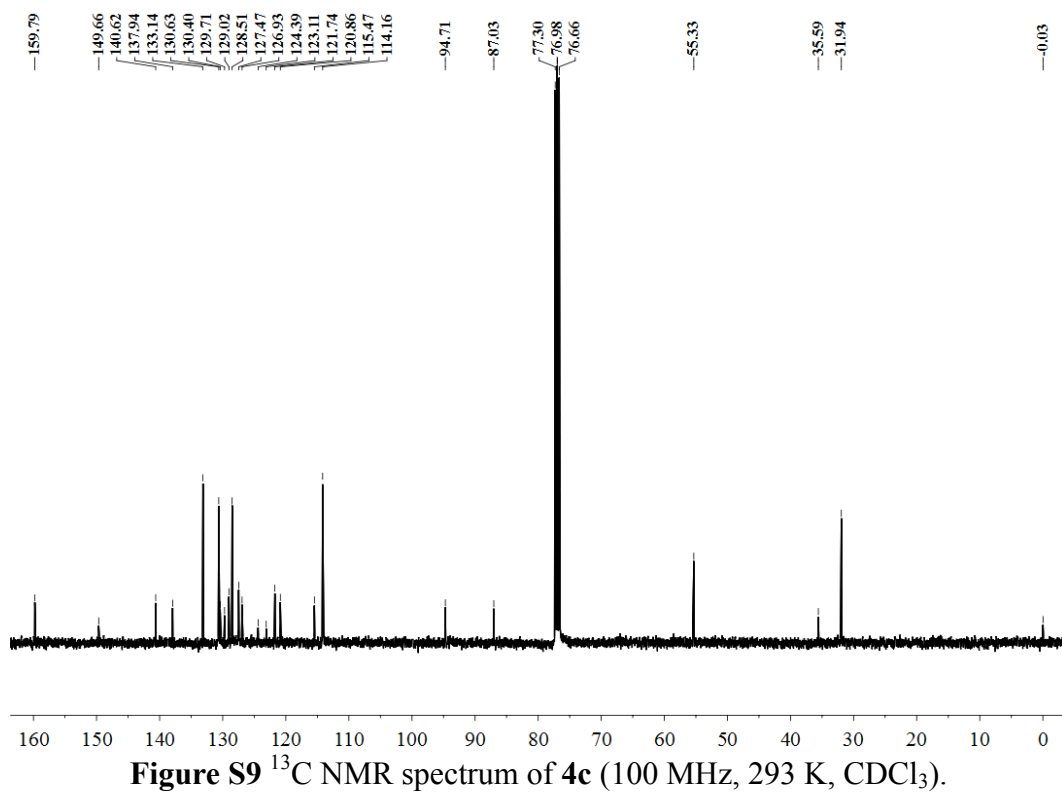


Figure S8 ^1H -NMR spectrum of **4c** (400 MHz, 293 K, CDCl_3).



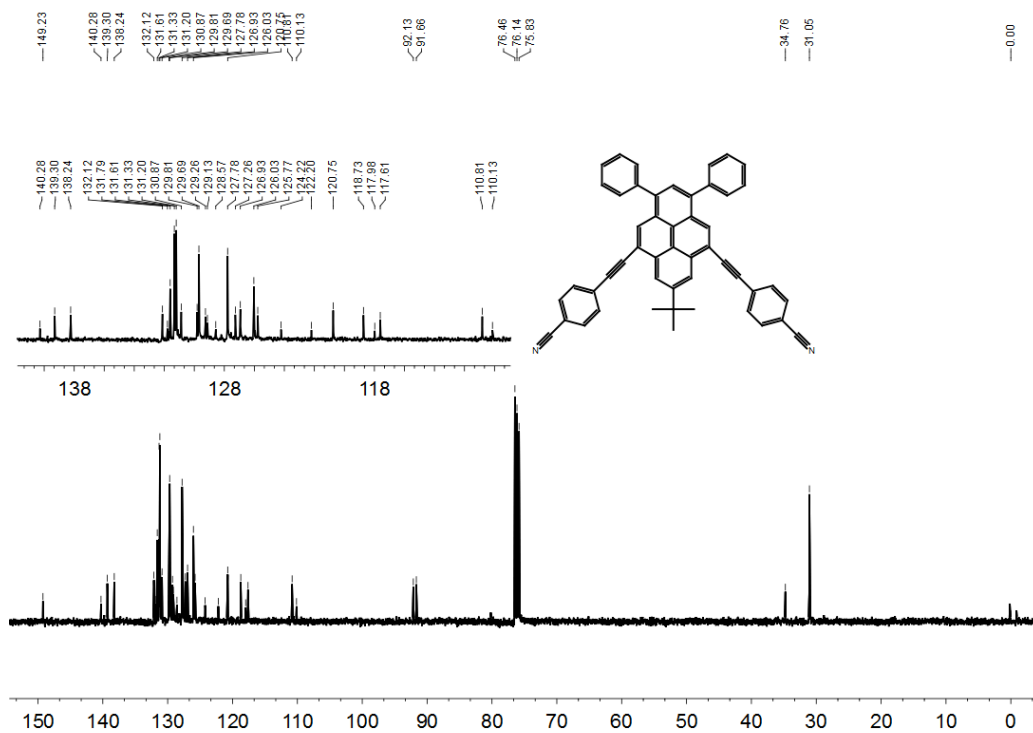


Figure S11 ¹³C NMR spectrum of **4d** (100 MHz, 293 K, CDCl₃).

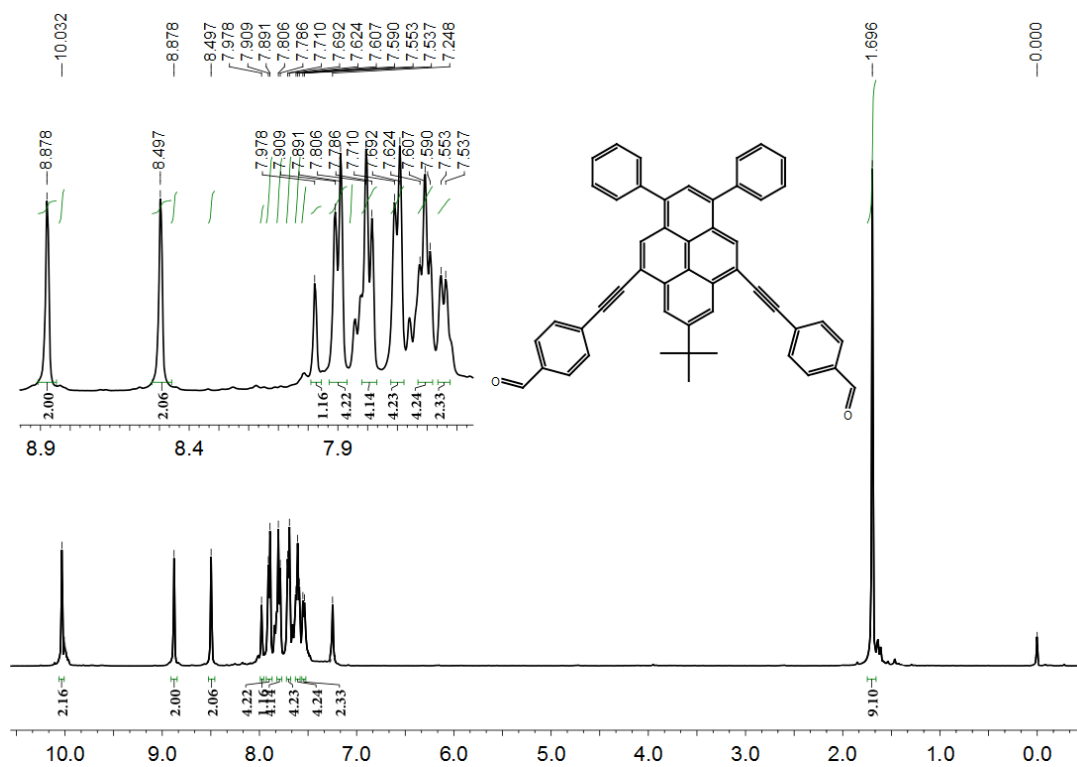


Figure S12 ¹H-NMR spectrum of **4e** (400 MHz, 293 K, CDCl₃).

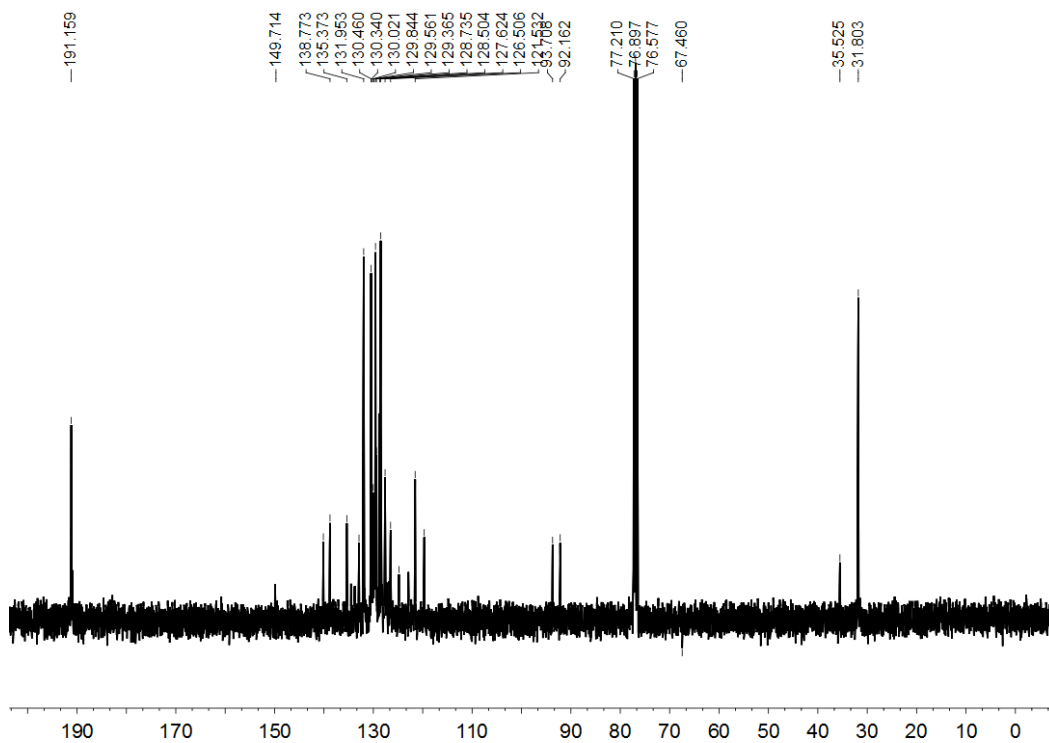


Figure S13 ^{13}C NMR spectrum of **4e** (100 MHz, 293 K, CDCl_3).

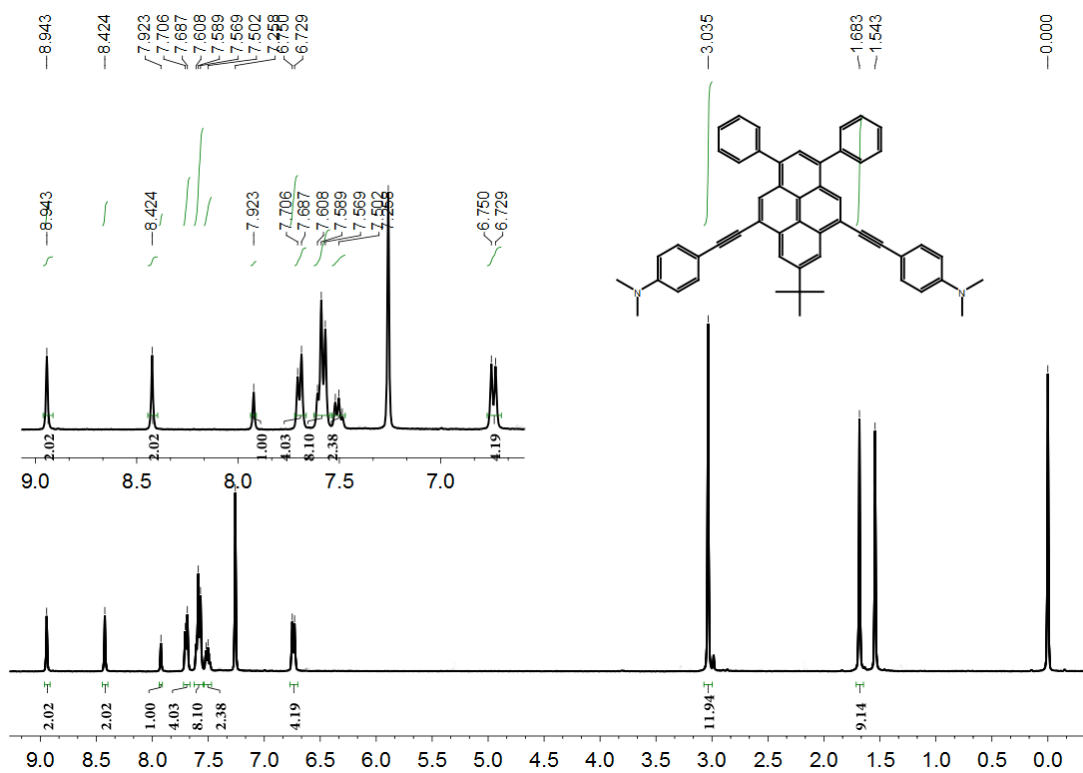


Figure S14 ^1H -NMR spectrum of **4f** (400 MHz, 293 K, CDCl_3).

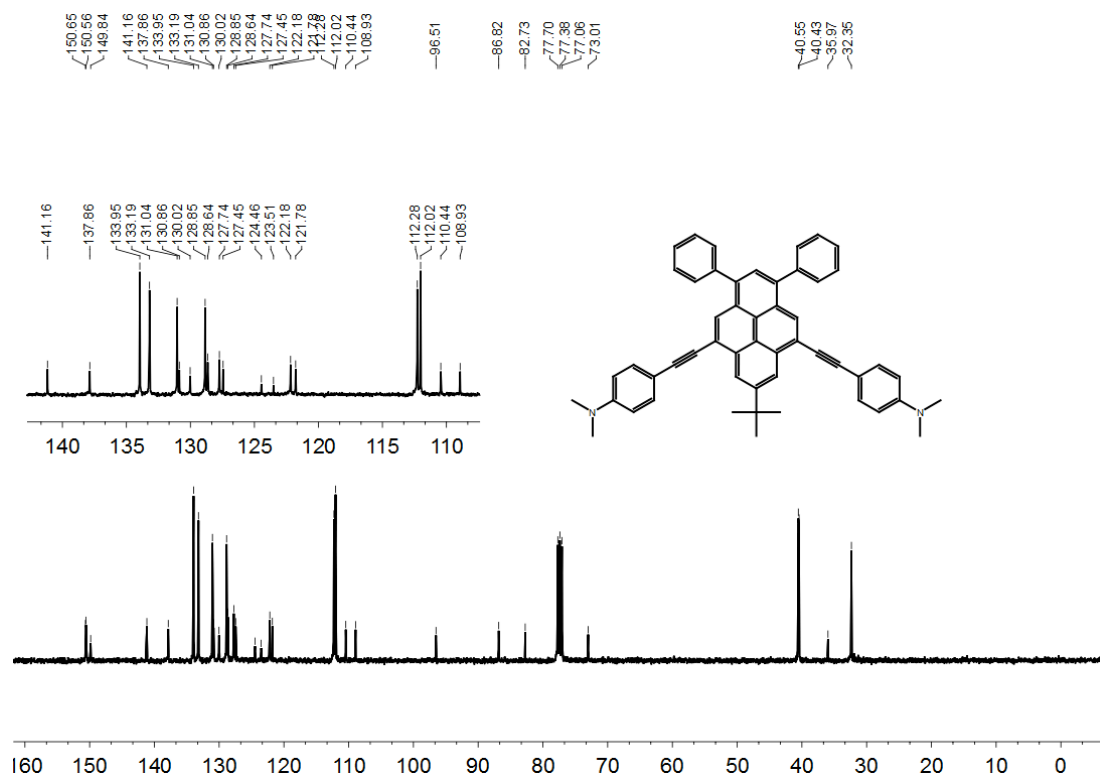


Figure S15 ^{13}C NMR spectrum of **4f** (100 MHz, 293 K, CDCl_3).

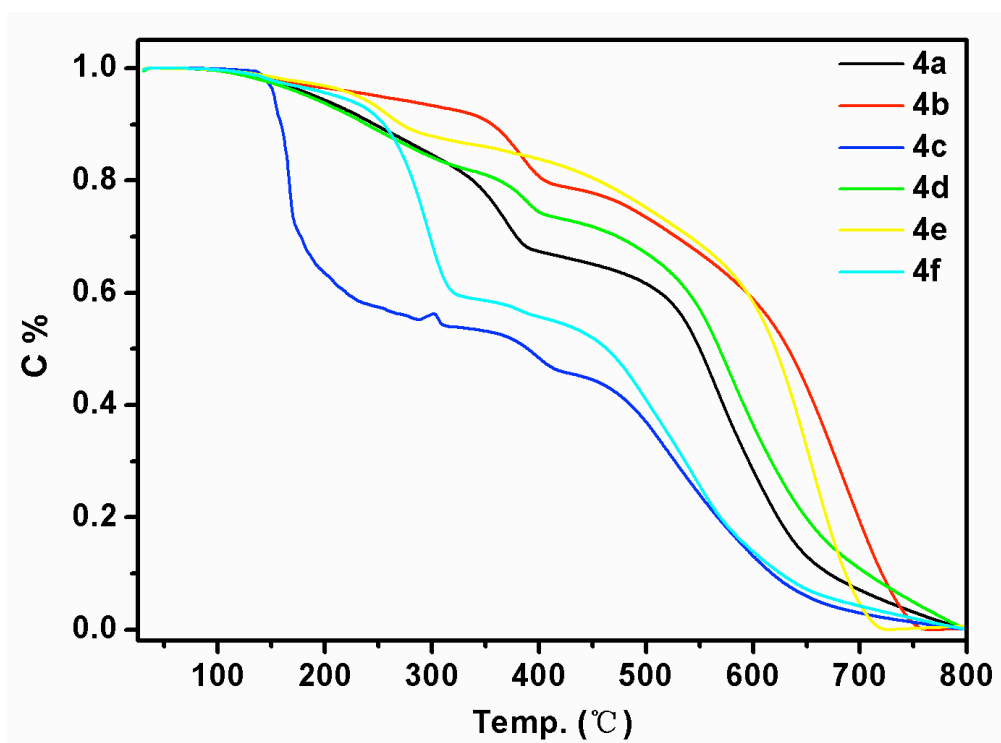


Figure S16 TGA thermograms of compounds **4**.

Table S1 Crystal data and structure refinement details for compound **4c**.^[a, b]

Comp.	4c
Empirical formula	C ₅₀ H ₃₈ O ₂
Formula weight	670.80
Crystal system	Monoclinic
Space group	<i>Cc</i>
<i>a</i> [Å]	16.3212 (13)
<i>b</i> [Å]	13.2595 (11)
<i>c</i> [Å]	18.230 (2)
α [°]	90.00
β [°]	115.0330 (12)
γ [°]	90.00
Volume[Å ³]	3574.6 (6)
<i>Z</i>	4
Crystal size[mm ³]	0.77 × 0.24 × 0.13
D _{calcd} [Mg/m ³]	1.246
temperature [K]	150 (2)
Measured reflns	21169
unique reflns	10490
obsd reflns	8919
parameters	474
<i>R</i> (int)	0.018
<i>R</i> [<i>I</i> > 2σ(<i>I</i>)] ^[a]	0.061
<i>wR</i> 2[all data] ^[b]	0.175
GOF on <i>F</i> ²	1.02

^[a] $R_1 = \sum ||F_o| - |F_c||$ (based on reflections with $F_o^2 > 2\sigma F^2$) ^[b] $wR_2 = [\sum [w(F_o^2 - F_c^2)^2] / \sum [w(F_o^2)^2]]^{1/2}$; $w = 1/[\sigma^2(F_o^2) + (0.095P)^2]$; $P = [\max(F_o^2, 0) + 2F_c^2]/3$ (also with $F_o^2 > 2\sigma F^2$)

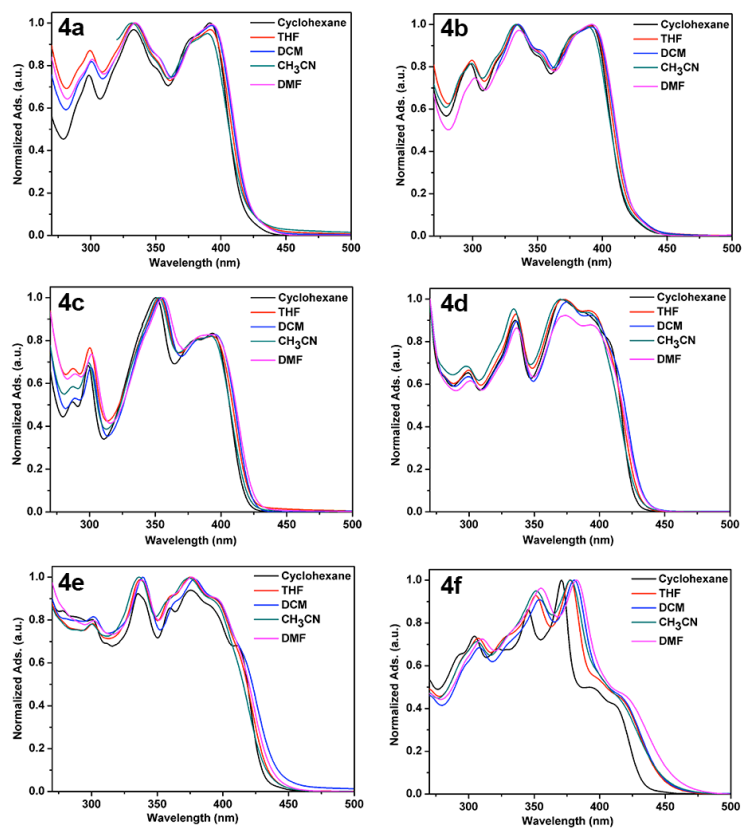


Figure S17 Absorption spectra of 4a–e recorded in different solvents.

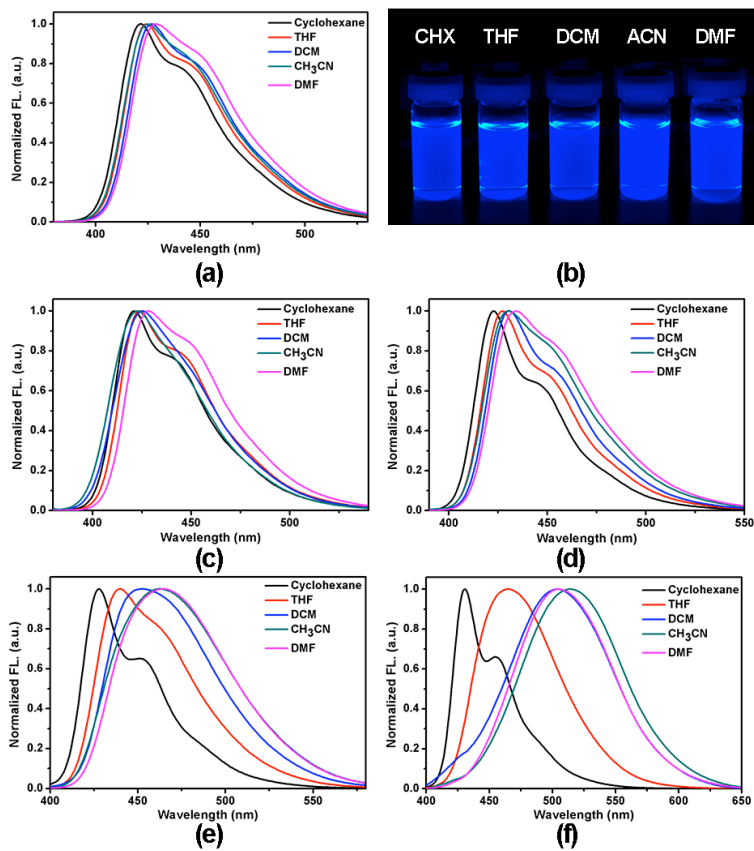


Figure S18 Emission spectra of 4a–e recorded in different solvents.

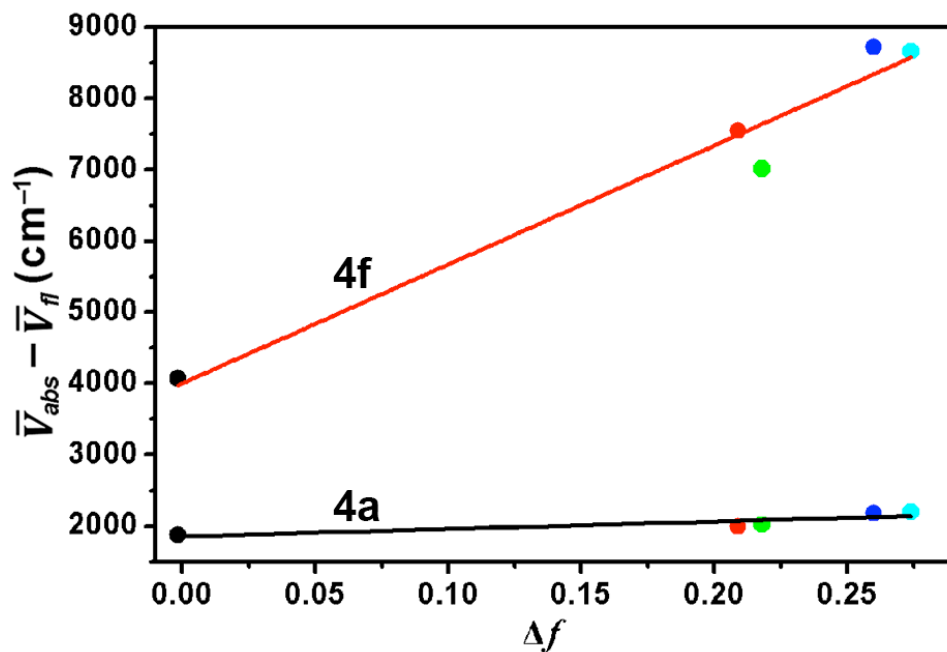


Figure S19 Lippert-Mataga plots for compounds 4a and 4f.

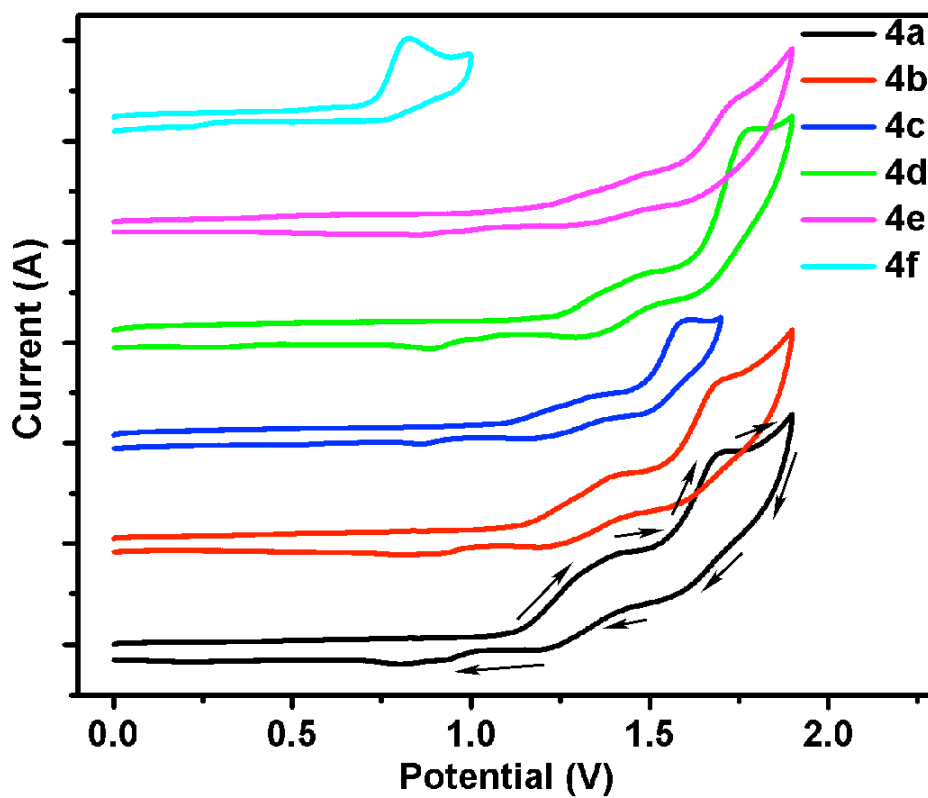


Figure S20 Cyclic voltammograms of fluorophores 4 in ferrocene in CH_2Cl_2 solution, scan rate is 0.1 V/s.

DFT calculation data of 4

Table S2. atom coordinates and absolute energies for **4a**

Standard orientation:

Center Number	Atomic Number	Atomic Type	Coordinates (Angstroms)		
			X	Y	Z
1	6	0	0.012044	3.898020	0.056749
2	6	0	1.243065	3.240735	-0.053476
3	6	0	1.257401	1.819280	-0.028472
4	6	0	0.014184	1.113001	0.015988
5	6	0	-1.229117	1.817634	0.078259
6	6	0	-1.215589	3.234853	0.143652
7	6	0	2.469793	1.062668	0.008083
8	6	0	0.012334	-0.318060	-0.003847
9	6	0	1.235079	-1.052509	-0.012962
10	6	0	2.483515	-0.311827	0.017854
11	6	0	1.208436	-2.455163	-0.032344
12	1	0	2.159622	-2.972454	-0.038244
13	6	0	0.009634	-3.174880	-0.039158
14	6	0	-1.187141	-2.447871	-0.036820
15	6	0	-1.213727	-1.049279	-0.016554
16	6	0	-2.462911	-0.306207	-0.022899
17	6	0	-2.445181	1.066965	0.027665
18	1	0	-3.387324	1.601478	0.011503
19	1	0	3.414704	1.590299	0.054047
20	1	0	0.009444	4.983963	0.063161
21	1	0	-2.140501	-2.966418	-0.062559
22	6	0	-0.036863	-4.713320	-0.068993
23	6	0	-0.792412	-5.174271	-1.336317
24	1	0	-0.844858	-6.269151	-1.378003
25	1	0	-1.816551	-4.787329	-1.353660
26	1	0	-0.289085	-4.823147	-2.243501
27	6	0	-0.781744	-5.228319	1.188735
28	1	0	-0.837500	-6.323349	1.179243
29	1	0	-0.262002	-4.922651	2.102964
30	1	0	-1.804502	-4.843670	1.239766
31	6	0	1.365531	-5.348113	-0.081521
32	1	0	1.926874	-5.082708	-0.982556
33	1	0	1.953107	-5.040464	0.790803
34	1	0	1.273851	-6.439320	-0.060521
35	6	0	-3.710183	-0.991843	-0.088307
36	6	0	3.731360	-1.001225	0.065139

37	6	0	-4.779223	-1.570363	-0.140988
38	6	0	4.799890	-1.581208	0.105518
39	6	0	-6.038635	-2.237777	-0.196371
40	6	0	-6.191048	-3.527589	0.348876
41	6	0	-7.150293	-1.616423	-0.798214
42	6	0	-7.423300	-4.174569	0.291324
43	1	0	-5.337690	-4.009067	0.816269
44	6	0	-8.378853	-2.270732	-0.850523
45	1	0	-7.036318	-0.623311	-1.221281
46	6	0	-8.520200	-3.550025	-0.307445
47	1	0	-7.528569	-5.169338	0.716369
48	1	0	-9.228936	-1.781037	-1.318258
49	1	0	-9.479953	-4.057605	-0.350424
50	6	0	6.058572	-2.252970	0.158830
51	6	0	7.114864	-1.861442	-0.686181
52	6	0	6.263236	-3.318148	1.057041
53	6	0	8.341187	-2.520052	-0.630799
54	1	0	6.960615	-1.041701	-1.380836
55	6	0	7.492746	-3.971307	1.105539
56	1	0	5.452048	-3.621602	1.711444
57	6	0	8.534628	-3.575889	0.263184
58	1	0	9.148662	-2.208801	-1.288372
59	1	0	7.638737	-4.791231	1.803884
60	1	0	9.492479	-4.087274	0.303706
61	6	0	-2.452794	4.050081	0.288841
62	6	0	-3.331671	3.870479	1.370579
63	6	0	-2.743325	5.065334	-0.639671
64	6	0	-4.462279	4.674249	1.515053
65	1	0	-3.113274	3.110444	2.115307
66	6	0	-3.874276	5.867603	-0.496013
67	1	0	-2.083728	5.209662	-1.491043
68	6	0	-4.740105	5.674816	0.582123
69	1	0	-5.124109	4.520038	2.363386
70	1	0	-4.081038	6.641643	-1.230656
71	1	0	-5.621911	6.299595	0.695722
72	6	0	2.466947	4.069887	-0.196326
73	6	0	3.402541	3.851271	-1.223830
74	6	0	2.691622	5.147638	0.680562
75	6	0	4.516840	4.676875	-1.366327
76	1	0	3.236744	3.046720	-1.934351
77	6	0	3.806263	5.971797	0.538565
78	1	0	1.995283	5.321323	1.496365
79	6	0	4.725758	5.740088	-0.485911
80	1	0	5.219596	4.492384	-2.174748

81	1	0	3.960206	6.791931	1.235158
82	1	0	5.596280	6.380795	-0.597454

Total Energy (RB3LYP) = -1849.56216723 Hartree

Table S3. atom coordinates and absolute energies for **4b**

Standard orientation:

Center Number	Atomic Number	Atomic Type	Coordinates (Angstroms)		
			X	Y	Z
1	6	0	0.013239	4.091414	0.000167
2	6	0	1.240654	3.427602	-0.077861
3	6	0	1.253287	2.007210	-0.042934
4	6	0	0.009174	1.302297	0.001000
5	6	0	-1.233051	2.010931	0.044533
6	6	0	-1.216743	3.430182	0.078685
7	6	0	2.466335	1.252261	-0.011506
8	6	0	0.007440	-0.128547	0.001908
9	6	0	1.229165	-0.862110	0.000948
10	6	0	2.480734	-0.123378	0.010319
11	6	0	1.202100	-2.264733	0.003807
12	1	0	2.153705	-2.781119	0.006206
13	6	0	0.005679	-2.985217	0.004857
14	6	0	-1.192078	-2.257565	0.004169
15	6	0	-1.218789	-0.859668	0.004067
16	6	0	-2.468829	-0.115763	-0.007217
17	6	0	-2.449240	1.258978	0.013172
18	1	0	-3.391659	1.792239	-0.009184
19	1	0	3.410738	1.782045	0.009437
20	1	0	0.014379	5.177553	-0.000331
21	1	0	-2.144208	-2.777431	0.002886
22	6	0	-0.036817	-4.524621	0.006646
23	6	0	-0.782611	-5.018984	-1.255606
24	1	0	-0.831219	-6.114783	-1.264799
25	1	0	-1.808638	-4.639017	-1.298596
26	1	0	-0.268539	-4.693942	-2.167253
27	6	0	-0.783070	-5.016121	1.269709
28	1	0	-0.831308	-6.111914	1.281637
29	1	0	-0.269495	-4.688678	2.180788
30	1	0	-1.809266	-4.636483	1.311235
31	6	0	1.370629	-5.151518	0.007523
32	1	0	1.945187	-4.865289	-0.880882
33	1	0	1.944660	-4.863729	0.895803
34	1	0	1.285691	-6.244027	0.008500

35	6	0	-3.715906	-0.800602	-0.044533
36	6	0	3.725793	-0.812223	0.046700
37	6	0	-4.789400	-1.374039	-0.074227
38	6	0	4.797008	-1.389963	0.073132
39	6	0	-6.053676	-2.027984	-0.108301
40	6	0	-6.138989	-3.435586	-0.124914
41	6	0	-7.248499	-1.278394	-0.125441
42	6	0	-7.373758	-4.075365	-0.156885
43	1	0	-5.226148	-4.022538	-0.112422
44	6	0	-8.486894	-1.911042	-0.157524
45	1	0	-7.193406	-0.194640	-0.113691
46	6	0	-8.529679	-3.301503	-0.172539
47	1	0	-7.452848	-5.157392	-0.169734
48	1	0	-9.413088	-1.346055	-0.171113
49	6	0	6.057554	-2.051214	0.104219
50	6	0	7.256752	-1.308773	0.123939
51	6	0	6.134236	-3.459423	0.114918
52	6	0	8.491376	-1.948921	0.152918
53	1	0	7.208101	-0.224663	0.116696
54	6	0	7.365264	-4.106553	0.143764
55	1	0	5.217748	-4.040641	0.100099
56	6	0	8.525792	-3.339656	0.162181
57	1	0	9.420959	-1.389572	0.168479
58	1	0	7.437944	-5.189081	0.152056
59	6	0	-2.453314	4.253446	0.182322
60	6	0	-3.370825	4.074127	1.232141
61	6	0	-2.698881	5.277562	-0.747873
62	6	0	-4.498581	4.887252	1.342056
63	1	0	-3.184810	3.305239	1.976726
64	6	0	-3.827761	6.089015	-0.639139
65	1	0	-2.003996	5.424251	-1.570343
66	6	0	-4.732704	5.896527	0.406089
67	1	0	-5.190964	4.736431	2.166177
68	1	0	-4.001984	6.869889	-1.374782
69	1	0	-5.612175	6.528942	0.492155
70	6	0	2.479697	4.247084	-0.181935
71	6	0	3.396804	4.064197	-1.231504
72	6	0	2.728152	5.271151	0.747515
73	6	0	4.526839	4.874056	-1.342025
74	1	0	3.208728	3.295162	-1.975406
75	6	0	3.859339	6.079327	0.638175
76	1	0	2.033639	5.420366	1.569835
77	6	0	4.763754	5.883436	-0.406860
78	1	0	5.218857	4.720603	-2.165964

79	1	0	4.035785	6.860267	1.373219
80	1	0	5.645040	6.513263	-0.493358
81	9	0	-9.728428	-3.918227	-0.203168
82	9	0	9.720914	-3.963639	0.189768

Total Energy (RB3LYP) = -2048.02862445 Hartree

Table S4. atom coordinates and absolute energies for **4c**

Standard orientation:

Center Number	Atomic Number	Atomic Type	Coordinates (Angstroms)		
			X	Y	Z
1	6	0	0.011134	4.341969	0.000994
2	6	0	1.238769	3.678673	-0.076383
3	6	0	1.252469	2.258282	-0.036539
4	6	0	0.008046	1.553937	0.011937
5	6	0	-1.234873	2.261647	0.054608
6	6	0	-1.218879	3.681040	0.083585
7	6	0	2.465636	1.503513	-0.005356
8	6	0	0.006726	0.123073	0.017782
9	6	0	1.228712	-0.610048	0.016047
10	6	0	2.481110	0.127696	0.019885
11	6	0	1.202134	-2.012825	0.023293
12	1	0	2.154478	-2.527869	0.023972
13	6	0	0.005937	-2.733623	0.030753
14	6	0	-1.192042	-2.006462	0.030042
15	6	0	-1.219269	-0.608527	0.024952
16	6	0	-2.470606	0.133723	0.012679
17	6	0	-2.450741	1.508720	0.027512
18	1	0	-3.393547	2.041142	0.003783
19	1	0	3.410209	2.033093	0.011626
20	1	0	0.012003	5.428167	-0.003833
21	1	0	-2.144516	-2.525695	0.031517
22	6	0	-0.035523	-4.273129	0.036711
23	6	0	-0.781289	-4.771853	-1.223791
24	1	0	-0.829071	-5.867883	-1.230315
25	1	0	-1.807486	-4.392480	-1.266764
26	1	0	-0.268284	-4.448483	-2.136615
27	6	0	-0.780881	-4.762508	1.301227
28	1	0	-0.828167	-5.858474	1.316485
29	1	0	-0.267247	-4.431974	2.211181
30	1	0	-1.807232	-4.383554	1.342051

31	6	0	1.372408	-4.898572	0.039328
32	1	0	1.946518	-4.614174	-0.849801
33	1	0	1.946059	-4.606231	0.926310
34	1	0	1.288999	-5.991335	0.044278
35	6	0	-3.716113	-0.553596	-0.020205
36	6	0	3.724985	-0.562754	0.051658
37	6	0	-4.788417	-1.130411	-0.046849
38	6	0	4.796209	-1.141750	0.071680
39	6	0	-6.050637	-1.786136	-0.088614
40	6	0	-6.141806	-3.189217	-0.086975
41	6	0	-7.251877	-1.042806	-0.129246
42	6	0	-7.375474	-3.836138	-0.125436
43	1	0	-5.230464	-3.778563	-0.053901
44	6	0	-8.481541	-1.678587	-0.168072
45	1	0	-7.202478	0.041594	-0.130807
46	6	0	-8.554773	-3.081056	-0.167983
47	1	0	-7.406050	-4.919530	-0.119457
48	1	0	-9.406475	-1.111383	-0.200749
49	6	0	6.056491	-1.802082	0.084482
50	6	0	7.261500	-1.062940	0.088822
51	6	0	6.142485	-3.205016	0.088800
52	6	0	8.489002	-1.702945	0.097253
53	1	0	7.215830	0.021656	0.084700
54	6	0	7.374535	-3.856686	0.097338
55	1	0	5.228612	-3.791400	0.083703
56	6	0	8.557523	-3.106245	0.102930
57	1	0	9.416928	-1.139735	0.099972
58	1	0	7.399893	-4.940293	0.095966
59	6	0	-2.454758	4.505432	0.184844
60	6	0	-3.371462	4.332853	1.236609
61	6	0	-2.700727	5.525753	-0.749538
62	6	0	-4.498326	5.147500	1.343770
63	1	0	-3.185729	3.567313	1.984637
64	6	0	-3.828385	6.339272	-0.643358
65	1	0	-2.006834	5.667619	-1.573706
66	6	0	-4.732664	6.152737	0.403483
67	1	0	-5.190203	5.000784	2.169109
68	1	0	-4.002302	7.116906	-1.382591
69	1	0	-5.611552	6.786314	0.487432
70	6	0	2.476421	4.499730	-0.185434
71	6	0	3.395178	4.311948	-1.232795
72	6	0	2.721784	5.531309	0.736512
73	6	0	4.523405	5.123581	-1.348014
74	1	0	3.209619	3.537266	-1.971342

75	6	0	3.850967	6.341765	0.622319
76	1	0	2.026148	5.684673	1.557109
77	6	0	4.757090	6.140438	-0.420081
78	1	0	5.216757	4.965671	-2.170032
79	1	0	4.024773	7.128422	1.351961
80	1	0	5.637151	6.771571	-0.510123
81	8	0	-9.810979	-3.607087	-0.207560
82	8	0	9.812806	-3.634467	0.112427
83	6	0	-9.949375	-5.019445	-0.190619
84	1	0	-9.532579	-5.454150	0.727522
85	1	0	-11.022340	-5.215073	-0.229047
86	1	0	-9.466776	-5.482252	-1.060887
87	6	0	9.951705	-5.046816	0.123083
88	1	0	11.025332	-5.240556	0.147056
89	1	0	9.484250	-5.491914	1.011042
90	1	0	9.519606	-5.501274	-0.778160

Total Energy (RB3LYP) = -2078.60890074 Hartree

Table S5. atom coordinates and absolute energies for **4d**

Standard orientation:

Center Number	Atomic Number	Atomic Type	Coordinates (Angstroms)		
			X	Y	Z
1	6	0	0.010313	-2.876414	0.005271
2	6	0	1.205746	-2.154147	0.000223
3	6	0	1.230871	-0.751719	-0.002657
4	6	0	0.008329	-0.019647	0.002255
5	6	0	-1.216761	-0.752539	0.008535
6	6	0	-1.188389	-2.150178	0.008610
7	6	0	2.480089	-0.009150	0.002852
8	6	0	0.008215	1.411308	0.001118
9	6	0	1.250475	2.119086	-0.048351
10	6	0	2.464571	1.366802	-0.020129
11	6	0	1.236283	3.539652	-0.084478
12	6	0	0.008575	4.202178	-0.000281
13	6	0	-1.219900	3.539024	0.084698
14	6	0	-1.234036	2.119550	0.050004
15	6	0	-2.449253	1.367062	0.022443
16	6	0	-2.466431	-0.008097	0.001377
17	1	0	-3.392174	1.899539	0.003713
18	1	0	2.157320	-2.670477	-0.000605
19	1	0	-2.139203	-2.672345	0.010568
20	1	0	3.408074	1.898277	-0.002569

21	1	0	0.008270	5.288169	-0.001032
22	6	0	2.474246	4.359259	-0.195558
23	6	0	2.726911	5.383651	0.732412
24	6	0	3.385400	4.175169	-1.250061
25	6	0	3.858050	6.190853	0.617055
26	1	0	2.036746	5.533610	1.558220
27	6	0	4.514830	4.984980	-1.366859
28	1	0	3.192634	3.406812	-1.993527
29	6	0	4.756756	5.994183	-0.432842
30	1	0	4.038743	6.971908	1.350774
31	1	0	5.202125	4.831818	-2.194672
32	1	0	5.637577	6.623806	-0.524204
33	6	0	-2.457623	4.359175	0.195094
34	6	0	-3.367983	4.177382	1.250658
35	6	0	-2.710829	5.381733	-0.734744
36	6	0	-4.497373	4.987406	1.366524
37	1	0	-3.174636	3.410635	1.995647
38	6	0	-3.841916	6.189142	-0.620330
39	1	0	-2.021186	5.530097	-1.561285
40	6	0	-4.739947	5.994638	0.430559
41	1	0	-5.184094	4.835951	2.195129
42	1	0	-4.023046	6.968702	-1.355528
43	1	0	-5.620685	6.624471	0.521237
44	6	0	-0.029958	-4.415862	0.006211
45	6	0	1.378406	-5.040726	0.005229
46	1	0	1.294767	-6.133153	0.006494
47	1	0	1.951327	-4.754638	-0.884342
48	1	0	1.953087	-4.752459	0.892988
49	6	0	-0.774217	-4.909212	1.269781
50	1	0	-0.260633	-4.581908	2.180865
51	1	0	-1.801330	-4.532115	1.312622
52	1	0	-0.820276	-6.004907	1.280543
53	6	0	-0.776561	-4.909474	-1.255974
54	1	0	-0.264430	-4.582621	-2.168023
55	1	0	-0.823219	-6.005172	-1.266369
56	1	0	-1.803486	-4.531589	-1.296965
57	6	0	3.727434	-0.691966	0.036819
58	6	0	-3.714183	-0.689806	-0.032708
59	6	0	4.800713	-1.266628	0.063028
60	6	0	-4.789151	-1.261494	-0.057994
61	6	0	6.062099	-1.920710	0.091557
62	6	0	6.143864	-3.329567	0.097606
63	6	0	7.257672	-1.170820	0.113588
64	6	0	7.375853	-3.966914	0.123804

65	1	0	5.229702	-3.914007	0.081145
66	6	0	8.490800	-1.805913	0.139923
67	1	0	7.202863	-0.087189	0.110031
68	6	0	8.561193	-3.210494	0.144981
69	1	0	7.432060	-5.050630	0.127981
70	1	0	9.406482	-1.223788	0.156778
71	6	0	-6.053743	-1.909081	-0.091274
72	6	0	-6.143495	-3.317331	-0.106717
73	6	0	-7.245323	-1.152596	-0.108601
74	6	0	-7.378847	-3.947855	-0.137982
75	1	0	-5.232742	-3.907110	-0.093721
76	6	0	-8.481863	-1.780748	-0.139922
77	1	0	-7.184581	-0.069341	-0.097586
78	6	0	-8.560011	-3.184862	-0.154668
79	1	0	-7.440933	-5.031192	-0.149562
80	1	0	-9.394317	-1.193491	-0.153205
81	6	0	9.833830	-3.867335	0.171421
82	6	0	-9.836164	-3.834588	-0.186250
83	7	0	10.867855	-4.400938	0.192540
84	7	0	-10.873029	-4.362462	-0.211550

Total Energy (RB3LYP) = -2034.04873800 Hartree

Table S6. atom coordinates and absolute energies for **4e**

Standard orientation:

Center Number	Atomic Number	Atomic Type	Coordinates (Angstroms)		
			X	Y	Z
1	6	0	0.010393	-2.793115	-0.034350
2	6	0	-1.189759	-2.077402	-0.011754
3	6	0	-1.223515	-0.675373	0.002402
4	6	0	-0.005827	0.064190	-0.006575
5	6	0	1.223520	-0.660940	-0.028311
6	6	0	1.204603	-2.059419	-0.041884
7	6	0	-2.477905	0.058576	0.006892
8	6	0	-0.013626	1.494674	0.004244
9	6	0	-1.260221	2.194337	0.068220
10	6	0	-2.470165	1.434881	0.038344
11	6	0	-1.252234	3.614287	0.113519
12	6	0	-0.030202	4.284674	0.018420
13	6	0	1.201829	3.628408	-0.080963
14	6	0	1.223293	2.209974	-0.053214

15	6	0	2.444234	1.463965	-0.041327
16	6	0	2.467484	0.090759	-0.026486
17	1	0	3.384311	2.002067	-0.028328
18	1	0	-2.138472	-2.599553	-0.009346
19	1	0	2.159263	-2.574287	-0.060052
20	1	0	-3.416871	1.960799	0.027938
21	1	0	-0.037077	5.370715	0.025946
22	6	0	-2.494061	4.426005	0.247194
23	6	0	-2.762763	5.459275	-0.665547
24	6	0	-3.389362	4.225249	1.311473
25	6	0	-3.896786	6.259045	-0.526549
26	1	0	-2.083691	5.621178	-1.498323
27	6	0	-4.521206	5.027989	1.452559
28	1	0	-3.182794	3.448899	2.042915
29	6	0	-4.780416	6.046078	0.533007
30	1	0	-4.091891	7.046275	-1.249998
31	1	0	-5.195562	4.863305	2.288805
32	1	0	-5.663137	6.670130	0.643002
33	6	0	2.435568	4.453646	-0.202652
34	6	0	3.363993	4.241808	-1.236726
35	6	0	2.672068	5.505810	0.698232
36	6	0	4.491086	5.053214	-1.361915
37	1	0	3.186860	3.449559	-1.958620
38	6	0	3.800180	6.316066	0.573652
39	1	0	1.973230	5.673905	1.513032
40	6	0	4.714653	6.092570	-0.456863
41	1	0	5.192981	4.876027	-2.172560
42	1	0	3.966286	7.119979	1.285870
43	1	0	5.594016	6.723248	-0.555108
44	6	0	0.055625	-4.332489	-0.061139
45	6	0	-1.350456	-4.962173	-0.007576
46	1	0	-1.262444	-6.054114	-0.010283
47	1	0	-1.892082	-4.675257	0.900560
48	1	0	-1.958365	-4.679031	-0.874633
49	6	0	0.745427	-4.802747	-1.364408
50	1	0	0.187787	-4.468292	-2.246613
51	1	0	1.766437	-4.417507	-1.449280
52	1	0	0.799670	-5.897600	-1.392211
53	6	0	0.859544	-4.843038	1.159024
54	1	0	0.375961	-4.550871	2.098094
55	1	0	0.927823	-5.937118	1.136978
56	1	0	1.879918	-4.446026	1.170802
57	6	0	-3.720796	-0.634302	-0.027225
58	6	0	3.720455	-0.590828	-0.001373

59	6	0	-4.789458	-1.217989	-0.053680
60	6	0	4.794977	-1.161891	0.011160
61	6	0	-6.050518	-1.875285	-0.087265
62	6	0	-6.127946	-3.279089	-0.239626
63	6	0	-7.245603	-1.133199	0.030193
64	6	0	-7.358256	-3.916039	-0.269617
65	1	0	-5.209416	-3.850526	-0.330704
66	6	0	-8.473979	-1.779955	-0.004942
67	1	0	-7.188988	-0.055397	0.144030
68	6	0	-8.544328	-3.173254	-0.153884
69	1	0	-7.430700	-4.993457	-0.382046
70	1	0	-9.392866	-1.204053	0.083458
71	6	0	6.055491	-1.827278	0.034984
72	6	0	6.307705	-2.849409	0.977081
73	6	0	7.066217	-1.475099	-0.882408
74	6	0	7.533292	-3.497498	0.997040
75	1	0	5.529438	-3.117328	1.684707
76	6	0	8.292390	-2.128436	-0.854370
77	1	0	6.873264	-0.691313	-1.607748
78	6	0	8.536994	-3.142998	0.080996
79	1	0	7.741039	-4.284408	1.715723
80	1	0	9.070243	-1.853808	-1.563827
81	6	0	-9.859352	-3.851239	-0.187880
82	1	0	-10.735740	-3.171947	-0.093847
83	6	0	9.846594	-3.833322	0.098072
84	1	0	10.575677	-3.469069	-0.659735
85	8	0	-10.017424	-5.052329	-0.304893
86	8	0	10.145252	-4.730816	0.862917

Total Energy (RB3LYP) = -2076.21215112 Hartree

Table S7. atom coordinates and absolute energies for **4f**

Standard orientation:

Center Number	Atomic Number	Atomic Type	Coordinates (Angstroms)		
			X	Y	Z
1	6	0	-0.005811	-2.604415	-0.014979
2	6	0	-1.202080	-1.883805	-0.005107
3	6	0	-1.228720	-0.481063	0.000950
4	6	0	-0.006621	0.252048	-0.005460
5	6	0	1.219474	-0.479342	-0.016768
6	6	0	1.192209	-1.877312	-0.020035
7	6	0	-2.482089	0.255819	-0.000015
8	6	0	-0.007848	1.682935	-0.001293

9	6	0	-1.252322	2.386972	0.051166
10	6	0	-2.465417	1.632113	0.024690
11	6	0	-1.238452	3.807638	0.089540
12	6	0	-0.010958	4.470682	0.006786
13	6	0	1.218579	3.809784	-0.080152
14	6	0	1.235231	2.390094	-0.050205
15	6	0	2.451000	1.637299	-0.028586
16	6	0	2.471917	0.261823	-0.012080
17	1	0	3.394021	2.169650	-0.010525
18	1	0	-2.154711	-2.398513	-0.003152
19	1	0	2.144996	-2.396149	-0.026093
20	1	0	-3.410054	2.161655	0.009562
21	1	0	-0.011666	5.556978	0.010371
22	6	0	-2.475566	4.628768	0.202912
23	6	0	-2.724671	5.661159	-0.717360
24	6	0	-3.391153	4.440770	1.253080
25	6	0	-3.852799	6.472306	-0.598299
26	1	0	-2.032107	5.814514	-1.540580
27	6	0	-4.518740	5.252649	1.373012
28	1	0	-3.204003	3.664320	1.989367
29	6	0	-4.755346	6.270776	0.447243
30	1	0	-4.028640	7.259737	-1.326722
31	1	0	-5.209435	5.093598	2.197133
32	1	0	-5.634774	6.902321	0.541107
33	6	0	2.453824	4.634524	-0.188343
34	6	0	3.369088	4.456300	-1.240454
35	6	0	2.701255	5.660641	0.739366
36	6	0	4.494963	5.271375	-1.354984
37	1	0	3.183028	3.685045	-1.982469
38	6	0	3.827634	6.474976	0.625707
39	1	0	2.008781	5.806619	1.564017
40	6	0	4.730001	6.283067	-0.421813
41	1	0	5.185464	5.119906	-2.180694
42	1	0	4.002247	7.257385	1.359816
43	1	0	5.608038	6.917151	-0.511489
44	6	0	0.036382	-4.143906	-0.020331
45	6	0	-1.371098	-4.770623	-0.015116
46	1	0	-1.286455	-5.863369	-0.019180
47	1	0	-1.941187	-4.485843	0.876549
48	1	0	-1.950081	-4.479902	-0.899116
49	6	0	0.775840	-4.633356	-1.288116
50	1	0	0.257082	-4.303824	-2.195552
51	1	0	1.801582	-4.253245	-1.334391
52	1	0	0.823968	-5.729352	-1.302692

53	6	0	0.789065	-4.641381	1.236582
54	1	0	0.279617	-4.318126	2.151521
55	1	0	0.838000	-5.737414	1.243366
56	1	0	1.814995	-4.260759	1.274678
57	6	0	-3.725373	-0.434313	-0.031568
58	6	0	3.716506	-0.425901	0.013545
59	6	0	-4.798378	-1.011393	-0.056254
60	6	0	4.790233	-1.002015	0.030745
61	6	0	-6.059590	-1.665444	-0.086879
62	6	0	-6.161377	-3.070718	-0.099911
63	6	0	-7.262068	-0.930482	-0.099605
64	6	0	-7.391927	-3.709423	-0.128013
65	1	0	-5.253356	-3.666527	-0.083361
66	6	0	-8.497227	-1.559669	-0.127948
67	1	0	-7.216858	0.154454	-0.083410
68	6	0	-8.600042	-2.971567	-0.152826
69	1	0	-7.412136	-4.792602	-0.130064
70	1	0	-9.389779	-0.945676	-0.130183
71	6	0	6.053063	-1.653447	0.047314
72	6	0	6.158260	-3.057003	0.112576
73	6	0	7.254110	-0.917254	0.004254
74	6	0	7.390248	-3.693214	0.129478
75	1	0	5.251596	-3.653586	0.155063
76	6	0	8.490809	-1.543867	0.020218
77	1	0	7.206506	0.166868	-0.038112
78	6	0	8.596993	-2.954729	0.073746
79	1	0	7.412666	-4.774805	0.187174
80	1	0	9.381973	-0.928531	-0.007724
81	7	0	-9.831312	-3.604166	-0.206399
82	7	0	9.829849	-3.586330	0.064928
83	6	0	-9.905220	-5.047641	-0.059277
84	1	0	-10.946797	-5.362645	-0.144892
85	1	0	-9.339491	-5.555442	-0.850262
86	1	0	-9.519237	-5.396188	0.911648
87	6	0	-11.047886	-2.823435	-0.062123
88	1	0	-11.910588	-3.486018	-0.152873
89	1	0	-11.110217	-2.308757	0.909685
90	1	0	-11.127628	-2.066074	-0.851755
91	6	0	11.043962	-2.795807	0.171861
92	1	0	11.100408	-2.228080	1.114031
93	1	0	11.908582	-3.460193	0.121752
94	1	0	11.125580	-2.082977	-0.658004
95	6	0	9.905326	-5.018975	0.294423
96	1	0	9.348339	-5.572444	-0.471788

97	1	0	10.948322	-5.335599	0.236917
98	1	0	9.510481	-5.312192	1.279865

Total Energy (RB3LYP) = -2117.49946072 Hartree

checkCIF/PLATON report

You have not supplied any structure factors. As a result the full set of tests cannot be run.

THIS REPORT IS FOR GUIDANCE ONLY. IF USED AS PART OF A REVIEW PROCEDURE FOR PUBLICATION, IT SHOULD NOT REPLACE THE EXPERTISE OF AN EXPERIENCED CRYSTALLOGRAPHIC REFEREE.

No syntax errors found. CIF dictionary Interpreting this report

Datablock: 4c

Bond precision: C-C = 0.0041 A Wavelength=0.71073

Cell: a=16.3212(13) b=13.2595(11) c=18.230(2)
 alpha=90 beta=115.0330(12) gamma=90

Temperature: 150 K

	Calculated	Reported
Volume	3574.6(6)	3574.6(6)
Space group	C c	C c
Hall group	C -2yc	C -2yc
Moiety formula	C50 H38 O2	C50 H38 O2
Sum formula	C50 H38 O2	C50 H38 O2
Mr	670.80	670.80
Dx, g cm ⁻³	1.247	1.246
Z	4	4
Mu (mm ⁻¹)	0.074	0.074
F000	1416.0	1416.0
F000'	1416.57	
h,k,lmax	23,18,26	23,18,26
Nref	10915[5462]	10490
Tmin,Tmax	0.979,0.990	0.945,0.990
Tmin'	0.945	

Correction method= # Reported T Limits: Tmin=0.945 Tmax=0.990
AbsCorr = MULTI-SCAN

Data completeness= 1.92/0.96 Theta(max)= 30.550

R(reflections)= 0.0612(8919) wR2(reflections)= 0.1750(10490)

S = 1.021 Npar= 474

The following ALERTS were generated. Each ALERT has the format
test-name_ALERT_alert-type_alert-level.
Click on the hyperlinks for more details of the test.

Alert level B

PLAT097_ALERT_2_B Large Reported Max. (Positive) Residual Density 0.85 eA-3
PLAT412_ALERT_2_B Short Intra XH3 .. XHn H27 .. H29C .. 1.72 Ang.

Alert level C

DIFMX02_ALERT_1_C The maximum difference density is > 0.1*ZMAX*0.75
The relevant atom site should be identified.
STRVA01_ALERT_4_C Flack test results are ambiguous.
From the CIF: `_refine_ls_abs_structure_Flack` 0.400
From the CIF: `_refine_ls_abs_structure_Flack_su` 0.500
PLAT094_ALERT_2_C Ratio of Maximum / Minimum Residual Density 3.21 Report
PLAT213_ALERT_2_C Atom C29 has ADP max/min Ratio 3.3 prolat
PLAT220_ALERT_2_C Non-Solvent Resd 1 C Ueq(max)/Ueq(min) Range 4.7 Ratio
PLAT222_ALERT_3_C Non-Solvent Resd 1 H Uiso(max)/Uiso(min) Range 5.1 Ratio
PLAT230_ALERT_2_C Hirshfeld Test Diff for O1 -- C29 .. 7.0 s.u.
PLAT340_ALERT_3_C Low Bond Precision on C-C Bonds 0.00411 Ang.

Alert level G

PLAT032_ALERT_4_G Std. Uncertainty on Flack Parameter Value High . 0.500 Report
PLAT063_ALERT_4_G Crystal Size Likely too Large for Beam Size 0.77 mm
PLAT066_ALERT_1_G Predicted and Reported Tmin&Tmax Range Identical ? Check
PLAT072_ALERT_2_G SHELXL First Parameter in WGHT Unusually Large 0.11 Report
PLAT333_ALERT_2_G Check Large Av C6-Ring C-C Dist. C1 -C14 1.43 Ang.
PLAT333_ALERT_2_G Check Large Av C6-Ring C-C Dist. C1 -C10 1.43 Ang.
PLAT371_ALERT_2_G Long C(sp2)-C(sp1) Bond C8 - C21 .. 1.43 Ang.
PLAT371_ALERT_2_G Long C(sp2)-C(sp1) Bond C16 - C42 .. 1.43 Ang.
PLAT371_ALERT_2_G Long C(sp2)-C(sp1) Bond C22 - C23 .. 1.43 Ang.
PLAT371_ALERT_2_G Long C(sp2)-C(sp1) Bond C43 - C44 .. 1.43 Ang.
PLAT933_ALERT_2_G Number of OMIT Records in Embedded .res File ... 4 Note

- 0 **ALERT level A** = Most likely a serious problem - resolve or explain
2 **ALERT level B** = A potentially serious problem, consider carefully
8 **ALERT level C** = Check. Ensure it is not caused by an omission or oversight
11 **ALERT level G** = General information/check it is not something unexpected
- 2 ALERT type 1 CIF construction/syntax error, inconsistent or missing data
14 ALERT type 2 Indicator that the structure model may be wrong or deficient
2 ALERT type 3 Indicator that the structure quality may be low
3 ALERT type 4 Improvement, methodology, query or suggestion
0 ALERT type 5 Informative message, check
-
-

It is advisable to attempt to resolve as many as possible of the alerts in all categories. Often the minor alerts point to easily fixed oversights, errors and omissions in your CIF or refinement strategy, so attention to these fine details can be worthwhile. In order to resolve some of the more serious problems it may be necessary to carry out additional measurements or structure refinements. However, the purpose of your study may justify the reported deviations and the more serious of these should normally be commented upon in the discussion or experimental section of a paper or in the "special_details" fields of the CIF. checkCIF was carefully designed to identify outliers and unusual parameters, but every test has its limitations and alerts that are not important in a particular case may appear. Conversely, the absence of alerts does not guarantee there are no aspects of the results needing attention. It is up to the individual to critically assess their own results and, if necessary, seek expert advice.

Publication of your CIF in IUCr journals

A basic structural check has been run on your CIF. These basic checks will be run on all CIFs submitted for publication in IUCr journals (*Acta Crystallographica*, *Journal of Applied Crystallography*, *Journal of Synchrotron Radiation*); however, if you intend to submit to *Acta Crystallographica Section C* or *E* or *IUCrData*, you should make sure that full publication checks are run on the final version of your CIF prior to submission.

Publication of your CIF in other journals

Please refer to the *Notes for Authors* of the relevant journal for any special instructions relating to CIF submission.

PLATON version of 27/03/2017; check.def file version of 24/03/2017

